

CHAPTER 2

RESULTS AND DISCUSSION

2.1 Characterization of Pyrimidine Based Ligands

The ligands [L1 – L6] were prepared by reacting 2-chloropyrimidine with ethylamine, aniline, *p*-toluidine, *m*-toluidine, *N*-methylaniline and piperidine respectively, as shown in Figure 2.1.

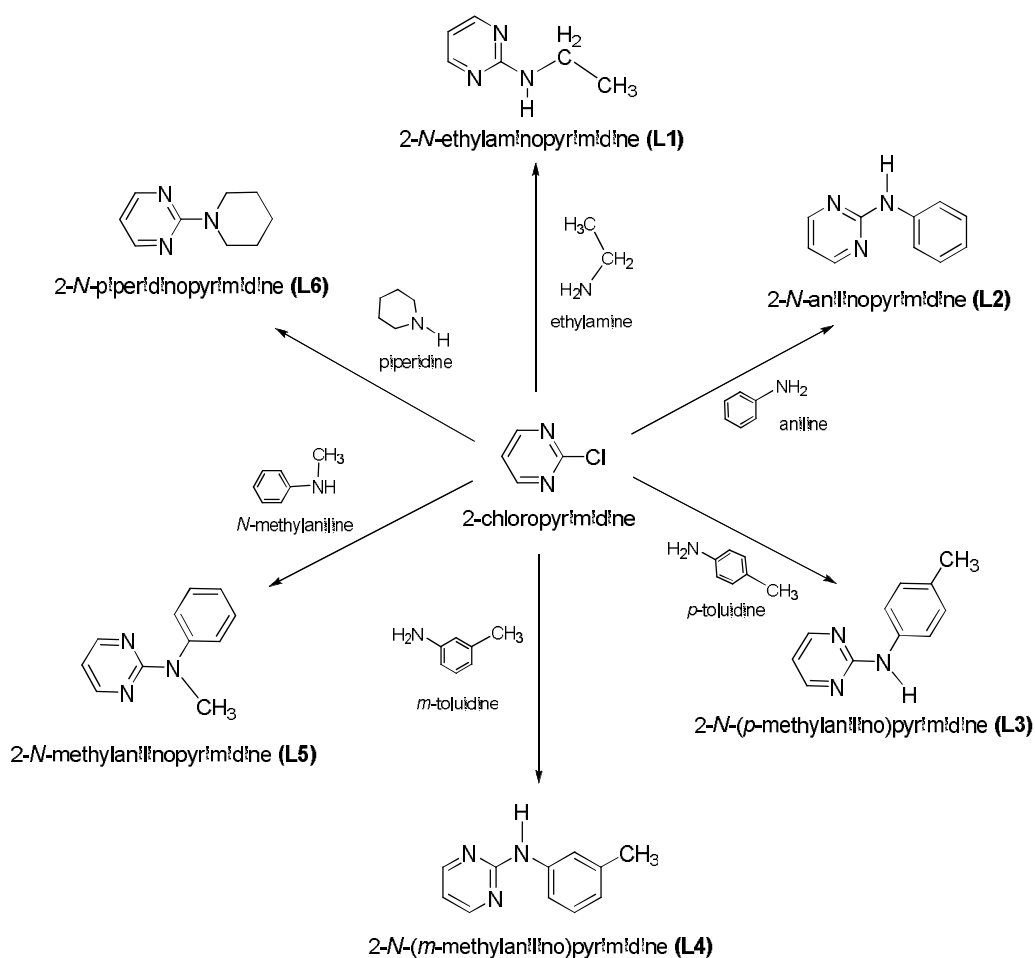
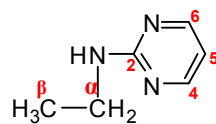


Figure 2.1 : Preparation of pyrimidine based ligands

2.1.1 2-N-Ethylaminopyrimidine (L1)

Treatment of 2-chloropyrimidine with ethylamine gave 86% yield of **L1**. **L1** showed an absorption band of medium intensity in its infrared spectrum at 3258 cm^{-1} which was due to N-H stretching. Medium absorption bands were observed indicating the presence of C=N and aromatic C=C stretches at 1595 cm^{-1} and 1534 cm^{-1} respectively. The GC-MS spectrum showed a molecular ion peak at m/z 123, which corresponded with the molecular formula $\text{C}_6\text{H}_9\text{N}_3$.



L1

The $^1\text{H-NMR}$, $^{13}\text{C-NMR}$ spectra of **L1** are as in the appendix. The $^1\text{H-NMR}$ spectrum of **L1** showed a doublet at δ 8.24 with J value of 4.9 Hz, which was due to H_4 and H_6 of pyrimidine ring. A triplet which observed at δ 6.47 with coupling constant of 4.9 Hz was attributed to H_5 of the pyrimidine ring. A broad peak at δ 5.17 was assigned to proton of the N-H group. A quintet recorded at δ 3.45 and a triplet at δ 1.21 with J value of 7.3 Hz, were due to protons resonance at H_α and H_β of the ethyl group.

The $^{13}\text{C-NMR}$ spectrum **L1** indicated the presence of 6 carbons which consist of one quaternary carbon, three methine carbons, one secondary carbon and one primary carbon in agreement with the molecular formula of **L1**. The signals at δ 162.29 δ 110.37 in the downfield region were attributed to the carbons of pyrimidine ring.

The spectrum showed a very low intensity absorption peak at δ 162.29, which was due to C₂ of the pyrimidine ring. A strong absorption peak at δ 158.01 was assigned to C₄ and C₆ of pyrimidine ring. One absorption peak at δ 110.37 was due to C₅ of pyrimidine ring. Meanwhile, medium absorption peaks were observed in the upfield region at δ 36.23 and δ 14.89, which were assigned to C and C of the ethyl group. The ¹H-NMR and ¹³C-NMR data of **L1** agreed with the proposed structure and the ¹H and ¹³C chemical shifts were shown in Table 2.1.

Table 2.1 : ¹H-NMR and ¹³C-NMR chemical shifts of 2-*N*-ethylaminopyrimidine (L1)

Proton / Carbon Number Assignments	Chemical Shift in ppm (δ) ^a	
	¹ H-NMR	¹³ C-NMR
2	-	162.29
4	8.24 (d, 2H)	158.01
5	6.47 (t, 1H)	110.37
6	8.24 (d, 2H)	158.01
	3.45 (q, 2H)	36.23
	1.21 (t, 3H)	14.89
N-H	5.17 (s, 1H)	-

^a s = singlet, d = doublet, t = triplet, q = quintet

2.1.2 2-*N*-Anilinopyrimidine (**L2**)

2-*N*-Anilinopyrimidine (**L2**) a well shaped colourless crystals were obtained when 2-chloropyrimidine was added to aniline and heated under reflux for 4 hours. The infrared spectrum of **L2** showed a strong band at 1578 cm^{-1} which was due to C=N stretching. Medium absorption band was observed, indicating the presence of aromatic C=C stretches at 1537 cm^{-1} . Weak absorption bands were observed at 3258 cm^{-1} and 1613 cm^{-1} which were due to N-H stretching and bending respectively. The GC-mass spectrum of **L2** showed a molecular ion peak at m/z 170 which is consistent with the molecular formula $\text{C}_{10}\text{H}_9\text{N}_3$.



L2

The $^1\text{H-NMR}$, $^{13}\text{C-NMR}$ spectra of **L2** are as in the appendix. The $^1\text{H-NMR}$ spectrum of **L2** showed a doublet at δ 8.40 with J value of 4.9 Hz, which was due to H_4 and H_6 of pyrimidine ring. A doublet at δ 7.59 with J value of 7.6 Hz was due to $\text{H}_{2\phi}$ and $\text{H}_{6\phi}$ of the benzene ring. A triplet was recorded at δ 7.34 with coupling constant of 7.6 Hz, was due to proton resonance at $\text{H}_{3\phi}$, $\text{H}_{5\phi}$ and N-H group. A triplet peak recorded at δ 7.03 with J value of 7.6 Hz was due to $\text{H}_{4\phi}$ of the benzene ring and another triplet was recorded at δ 6.69 with coupling constant of 4.9 Hz was due to proton resonance at H_5 of the pyrimidine ring.

The ^{13}C -NMR spectrum of **L2** showed a relatively low absorption peak at δ 160.21, which was due to C_2 of the pyrimidine ring. A strong peak at δ 157.98 was assigned to C_4 and C_6 of pyrimidine ring and a peak at δ 139.35 was due to $\text{C}_{1\phi}$ of benzene ring. Another strong absorption peak at δ 128.94 was assigned to $\text{C}_{2\phi}$ and $\text{C}_{6\phi}$ of benzene ring while a medium peak at δ 122.74 was due to $\text{C}_{4\phi}$ of benzene ring. Two absorption peaks at δ 119.53 and δ 112.52 were assigned to $\text{C}_{3\phi}$ and $\text{C}_{5\phi}$ of the benzene ring and C_5 of pyrimidine ring. The full proton and carbon assignments were summarized in Table 2.2.

Table 2.2 : ^1H -NMR and ^{13}C -NMR chemical shifts of 2-*N*-anilinopyrimidine (**L2**)

Proton / Carbon Number Assignments	Chemical Shift in ppm (δ) ^a	
	^1H -NMR	^{13}C -NMR
2	-	160.21
4	8.40 (d, 2H)	157.98
5	6.69 (t, 1H)	112.52
6	8.40 (d, 2H)	157.98
1 ϕ	-	139.35
2 ϕ	7.59 (d, 2H)	128.94
3 ϕ	7.34 (t, 3H)	119.53
4 ϕ	7.03 (t, 1H)	122.74
5 ϕ	7.34 (t, 3H)	119.53
6 ϕ	7.59 (d, 2H)	128.94
N-H	7.34 (t, 3H)	-

^a d = doublet, t = triplet

Recrystallization of **L2** in ethylacetate gave colourless crystals along with some unidentified brown material which were analyzed by X-ray diffraction. The crystal **L2** crystallizes in the triclinic system, *P* space group. There are two molecules in the asymmetric unit, with inter-ring dihedral angles of 31.1 (1) and 35.3 (1) $^{\circ}$. The bridging C6N6C bond angles are 128.2 (1) and 129.1 (1) $^{\circ}$. In the crystal, the two independent molecules are linked into a dimer by two N6H \cdots N hydrogen bonds. Figure 2.2 shows the thermal ellipsoids of **L2** at the 70% probability level, hydrogen atoms were drawn as spheres of arbitrary radius. The crystal system and refinement data are shown in Table 2.3. Selected hydrogen bonds shown in Table 2.4, indicate that intermolecular hydrogen bonds link the amino and pyrimidyl units.

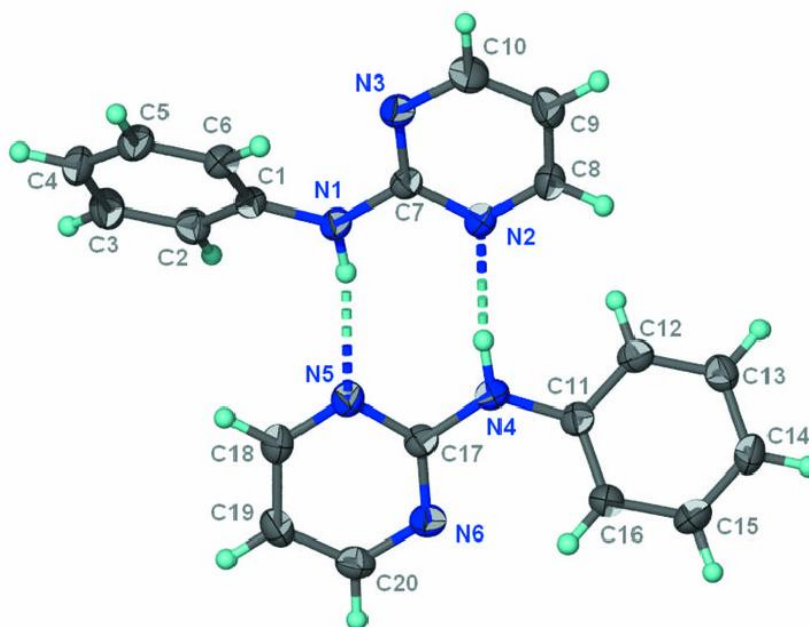


Figure 2.2 : ORTEP diagram of 2-N-anilinopyrimidine (L2)

Table 2.3 : Crystal data and structure refinement for 2-*N*-anilinopyrimidine (L2)

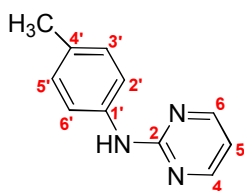
Identification code	<i>N</i> -(Pyrimidin-2-yl)aniline
Empirical formula	C ₁₀ H ₉ N ₃
Formula weight (g mol ⁻¹)	171.20
Colour	Colourless
Crystal system, space group	Triclinic, <i>P</i>
Unit cell dimensions	<i>a</i> = 8.8792 (2) Å <i>b</i> = 9.9382 (2) Å <i>c</i> = 10.2038 (2) Å = 93.186 (1) ^o = 103.665 (1) ^o = 97.780 (1) ^o
<i>V</i> (Å ³)	863.28 (3)
<i>Z</i>	4
<i>P</i> _{calc.} (mg m ⁻³)	1.317
Absorption coefficient (mm ⁻¹)	0.08
<i>F</i> ₀₀₀	360
Crystal size (mm)	0.35 x 0.20 x 0.10
θ _{max}	2.7 ó 28.3
Öh Ö	-11 to 11
Ök Ö	-12 to 12
Öl Ö	-13 to 12
Reflections collected / unique	8238/ 3950
<i>R</i> _{int}	0.020
Data / restraints / parameters	3950/ 2/ 243
Goodness-of-fit on <i>F</i> ²	1.03
Final <i>R</i> indices [<i>I</i> >2σ (<i>I</i>)]	0.039
<i>R</i> indices (all data)	0.108

Table 2.4 : Hydrogen-bond geometry (Å, °) for 2-*N*-anilinopyrimidine (L2)

<i>D</i> ó H... <i>A</i>	<i>D</i> ó H	H... <i>A</i>	<i>D</i> ... <i>A</i>	<i>D</i> ó H... <i>A</i>
N16H1...N5	0.89 (1)	2.10 (1)	2.972 (1)	164 (1)
N46H4...N2	0.89 (1)	2.15 (1)	3.020 (1)	165 (1)

2.1.3 2-*N*-(*p*-Methylanilino)pyrimidine (**L3**)

A 67% yield of 2-*N*-(*p*-methylanilino)pyrimidine, **L3** was obtained when an ethanolic mixture of 2-chloropyrimidine and *p*-toluidine were heated under reflux in an oil bath for about 5 hours. Compound **L3** showed two absorption bands of medium intensity in its infrared spectrum at 3258 cm⁻¹ and 1614 cm⁻¹ which were due to N-H stretching and bending respectively. Similar absorption bands were observed as in compound **L2** indicating the presence of C=N and C=C aromatic stretches, except that an additional strong absorption peak was observed at 817 cm⁻¹, indicating the para disubstitute ion in the benzene ring. The mass spectrum displayed [M⁺] peak at *m/z* 184 which is consistent with the molecular formula C₁₁H₁₁N₃.



L3

The ¹H-NMR, ¹³C-NMR spectra of **L3** are as in the appendix. The ¹H-NMR spectrum of **L3** showed a doublet at δ 8.39 with coupling constant of 4.6 Hz, which was due to H₄ and H₆ of pyrimidine ring. A doublet which was observed at δ 7.47 with *J* value of 6.4 Hz was due to H_{3_o} and H_{5_o} while another doublet peak was observed at δ 7.14 with *J* value of 8.3 Hz was due to H_{2_o} and H_{6_o} of the benzene ring. A triplet was recorded at δ 6.67 with coupling constant of 4.9 Hz, was due to proton resonance at H₅ of pyrimidine ring. A singlet peak was observed at δ 2.32 was due to protons of the δCH₃ group.

The ^{13}C -NMR spectrum of **L3** showed 8 carbon resonances having a total of 11 carbon atoms which consist of three quaternary carbons, seven methine carbons and one primary carbon, in agreement with the molecular formula of **L3**. A very low intensity absorption peak was observed at δ 160.91, which was due to C_2 of the pyrimidine ring. One peak at δ 157.99 was assigned to C_4 and C_6 of pyrimidine ring. A relatively low absorption peaks at δ 136.65 and δ 132.50 were assigned to $\text{C}_{1\phi}$ and $\text{C}_{4\phi}$ of benzene ring respectively. A strong absorption peak was observed at δ 129.45, which was assigned to $\text{C}_{3\phi}$ and $\text{C}_{5\phi}$ and a peak at δ 120.07 was due to $\text{C}_{2\phi}$ and $\text{C}_{6\phi}$ of benzene ring. Two peaks at δ 112.20 and δ 20.79 were due to C_5 of the pyrimidine ring and C of the methyl group. The ^1H -NMR and ^{13}C -NMR data of **L3** agreed with the proposed structure of **L3** as shown in Table 2.5.

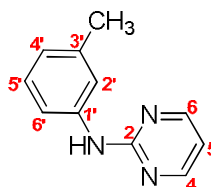
Table 2.5 : ^1H -NMR and ^{13}C -NMR chemical shifts of 2-*N*-(*p*-methylanilino)pyrimidine (L3**)**

Proton / Carbon Number Assignments	Chemical Shift in ppm (δ) ^a	
	^1H -NMR	^{13}C -NMR
2	-	160.91
4	8.39 (d, 2H)	157.99
5	6.67 (t, 1H)	112.20
6	8.39 (d, 2H)	157.99
1 ϕ	-	136.65
2 ϕ	7.14 (d, 2H)	120.07
3 ϕ	7.47 (d, 2H)	129.45
4 ϕ	-	132.50
5 ϕ	7.47 (d, 2H)	129.45
6 ϕ	7.14 (d, 2H)	120.07
- CH_3	2.32 (s, 3H)	20.79

^a s = singlet, d = doublet, t = triplet

2.1.4 2-*N*-(*m*-Methylanilino)pyrimidine (**L4**)

Treatment of 2-chloropyrimidine with *m*-toluidine in an ethanolic solution gave 58% yield of colourless crystals of **L4**, 2-*N*-(*m*-methylanilino)pyrimidine. The infrared spectrum of **L4** was almost identical to that of **L3**, whereby two medium absorption bands at 3257 cm⁻¹ and 1614 cm⁻¹ corresponding to N-H stretching and bending were observed. The presence of C=N and C=C aromatic stretching were recorded at 1573 cm⁻¹ and 1534 cm⁻¹ respectively. Two bands at 792 cm⁻¹ and 778 cm⁻¹ were observed, which were characteristic of meta disubstituted benzene ring. The GC-MS spectrum showed a molecular ion peak at *m/z* 184 which is in agreement with the molecular formula of C₁₁H₁₁N₃.



L4

The ¹H-NMR, ¹³C-NMR spectra of **L4** are as in the appendix. The ¹H-NMR spectrum of **L4** showed a doublet at δ 8.42 with *J* value of 4.9 Hz, which was due to H₄ and H₆ of pyrimidine ring. A doublet at δ 7.61 with coupling constant of 8.3 Hz was due to H_{2_o} and H_{6_o} of the benzene ring. A triplet peak was observed at δ 7.34 with *J* value of 7.6 Hz was due to H_{5_o} of the benzene ring, while another triplet was recorded at δ 7.05 with *J* value of 7.6 Hz was due to H₅ of pyrimidine ring. A doublet which was observed at δ 6.72 with coupling constant of 4.9 Hz was attributed to H_{4_o} of the benzene ring. A singlet peak was observed at δ 2.17 was due to protons of the δCH₃ group.

The ^{13}C -NMR spectrum showed a total of 11 carbon peaks. A very low intensity absorption peak was observed at δ 160.29, which was due to C_2 of the pyrimidine ring. A strong absorption peak was assigned at δ 157.98 was due to C_4 and C_6 of pyrimidine ring. Two peaks at δ 139.19 and δ 138.79 were assigned to $\text{C}_{1\phi}$ and $\text{C}_{3\phi}$ of benzene ring respectively. A relatively strong absorption peaks at δ 128.78 and δ 123.66 were assigned to $\text{C}_{5\phi}$ and $\text{C}_{2\phi}$ benzene ring respectively. One peak was observed at δ 120.17 was due to $\text{C}_{4\phi}$ of benzene ring while another two peaks at δ 116.71 and δ 112.41 were due to C_5 of the pyrimidine ring and $\text{C}_{6\phi}$ of the benzene ring respectively. In the upfield region, the absorption peak at δ 21.58 was observed which was due to the carbon resonance of the methyl group. The full proton and carbon assignments of **L4** were summarized in Table 2.6.

Table 2.6 : ^1H -NMR and ^{13}C -NMR chemical shifts of 2-*N*-(*m*-methylanilino)pyrimidine (L4**)**

Proton / Carbon Number Assignments	Chemical Shift in ppm (δ) ^a	
	^1H -NMR	^{13}C -NMR
2	-	160.29
4	8.42 (d, 2H)	157.98
5	7.05 (t, 1H)	116.71
6	8.42 (d, 2H)	157.98
1 ϕ	-	139.19
2 ϕ	7.61 (d, 1H)	123.66
3 ϕ	-	138.79
4 ϕ	6.72 (d, 1H)	120.17
5 ϕ	7.34 (t, 1H)	128.78
6 ϕ	7.61 (d, 1H)	112.41
- CH_3	2.17 (s, 3H)	21.58

^a s = singlet, d = doublet, t = triplet

Recrystallization of **L4** in ethylacetate gave colourless crystals along which were analyzed by X-ray diffraction method. Two independent molecules comprise the asymmetric unit, **L4**. These differ in terms of the relative orientations of the aromatic rings: the first is somewhat twisted, while the second is approximately planar [dihedral angles between the pyrimidine and phenyl rings = 39.00 (8) and 4.59 (11)^o]. Figure 2.3 shows an ORTEP diagram of **L4** at the 50% probability level. The crystal system and refinement data is shown in Table 2.7. It is noted that each of the N2 and N4 atoms forms a significant intermolecular C6H...N contact and that the contact formed in the second independent molecule is significantly shorter as shown in Table 2.8.

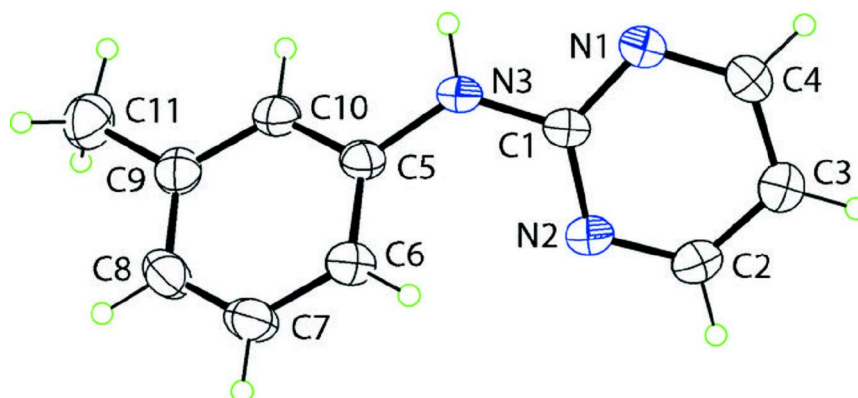


Figure 2.3 : ORTEP diagram of 2-*N*-(*m*-methylanilino)pyrimidine (L4**)**

Table 2.7 : Crystal data and structure refinement for 2-*N*-(*m*-methylanilino)pyrimidine (L4)

Identification code	<i>N</i> -(3-Methylphenyl)pyrimidin-2-amine
Empirical formula	C ₁₁ H ₁₁ N ₃
Formula weight (g mol ⁻¹)	185.23
Colour	Colourless
Crystal system, space group	Triclinic, <i>P</i>
Unit cell dimensions	<i>a</i> = 9.4461 (10) Å <i>b</i> = 10.0946 (11) Å <i>c</i> = 11.6266 (13) Å = 80.401 (1)° = 82.745 (2)° = 66.005 (1)°
<i>V</i> (Å ³)	996.55 (19)
<i>Z</i>	4
<i>P</i> _{calc.} (mg m ⁻³)	1.235
Absorption coefficient (mm ⁻¹)	0.08
<i>F</i> ₀₀₀	392
Crystal size (mm)	0.20 x 0.20 x 0.10
θ _{max}	4.4 ó 24.7
Öh Ö	-11 to 12
Ök Ö	-12 to 13
Öl Ö	-15 to 15
Reflections collected / unique	9569/ 4539
<i>R</i> _{int}	0.035
Data / restraints / parameters	4539/ 2/ 264
Goodness-of-fit on <i>F</i> ²	1.02
Final <i>R</i> indices [<i>I</i> > 2σ (<i>I</i>)]	0.051
<i>R</i> indices (all data)	0.167

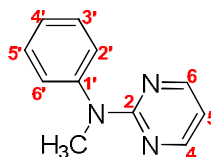
Table 2.8 : Hydrogen-bond geometry (Å, °) for 2-*N*-(*m*-methylanilino)pyrimidine (L4)

<i>D</i> ó H... <i>A</i>	<i>D</i> ó H	H... <i>A</i>	<i>D</i> ... <i>A</i>	<i>D</i> ó H... <i>A</i>
N3óH3...N2	0.86 (1)	2.19 (1)	3.0377 (19)	170 (2)
N6óH6...N1	0.87 (1)	2.45 (1)	3.2391 (19)	151 (2)
C6óH6...N1	0.93	2.55	2.961 (2)	107

Symmetry code: (i) óx + 1, óy + 2, óz

2.1.5 2-*N*-Methylanilinopyrimidine (**L5**)

The reaction of 2-chloropyrimidine with *N*-methylaniline gave 2-*N*-methylanilinopyrimidine, **L5**, a colourless crystals obtained with a yield of 56%. The infrared spectrum of compound **L5** showed a weak absorption band at 3036 cm⁻¹ which was due to the N-H stretching of the tertiary amine. Similar absorption band was observed as in compound **L2** indicating the presence of C=N at 1581 cm⁻¹. Medium absorption band was observed at 1550 cm⁻¹ which was due to the presence of aromatic C=C stretching. A weak absorption band was recorded at 1600 cm⁻¹ which was due to N-H bending. The spectrum showed a molecular ion peak at *m/z* 184, which corresponded with the molecular formula C₁₁H₁₁N₃.



L5

The ¹H-NMR, ¹³C-NMR spectra of **L5** are as in the appendix. The ¹H-NMR spectrum of **L5** showed a doublet at δ 8.32 with coupling constant of 8.3 Hz, which was due to H₄ and H₆ of pyrimidine ring. A multiplet at δ 7.20 ó 7.41 was assigned to H_{2_α}, H_{3_ø}, H_{4_α}, H_{5_ø} and H_{6_ø} of the benzene ring. A triplet was recorded at δ 6.54 with *J* value of 4.9 Hz, was due to proton resonance at H₅ of pyrimidine ring. A singlet peak was observed at δ 3.50 was due to protons of the óCH₃ group.

The ^{13}C -NMR spectrum **L5** indicated the presence of 11 carbons which consist of two quaternary carbons, eight methine carbons and one primary carbon in agreement with the molecular formula of **L5**. A very low absorption peak was observed at δ 162.79, which was due to C_2 of the pyrimidine ring. One absorption peak at δ 157.64 was assigned to C_4 and C_6 of pyrimidine ring. A peak was observed at δ 145.98 was assigned to $\text{C}_{1\phi}$ of benzene ring. A strong absorption peak at δ 129.18 was assigned to $\text{C}_{3\phi}$ and $\text{C}_{5\phi}$, whereas peak at δ 126.57 was assigned to $\text{C}_{4\phi}$ of the benzene ring. A relatively low absorption peak was recorded at δ 125.86 was due to C_5 of the pyrimidine ring, while another peak at δ 110.72 was due to $\text{C}_{2\phi}$ and $\text{C}_{6\phi}$ of the benzene ring. One absorption peak at δ 38.67 was assigned to carbon of the methyl group. The ^1H -NMR and ^{13}C -NMR data of **L5** agreed with the proposed structure and the chemical shifts were shown in Table 2.9.

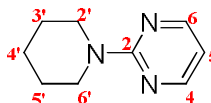
Table 2.9 : ^1H -NMR and ^{13}C -NMR chemical shifts of 2-*N*-methylanilinopyrimidine (L5**)**

Proton / Carbon Number Assignments	Chemical Shift in ppm (δ) ^a	
	^1H -NMR	^{13}C -NMR
2	-	162.79
4	8.32 (d, 2H)	157.64
5	6.54 (t, 1H)	125.86
6	8.32 (d, 2H)	157.64
1 ϕ	-	145.98
2 ϕ	7.20 δ 7.41 (m, 5H)	110.72
3 ϕ	7.20 δ 7.41(m, 5H)	129.18
4 ϕ	7.20 δ 7.41(m, 5H)	126.57
5 ϕ	7.20 δ 7.41(m, 5H)	129.18
6 ϕ	7.20 δ 7.41(m, 5H)	110.72
- CH_3	3.50 (s, 3H)	38.67

^a s = singlet, d = doublet, t = triplet, m = multiplet

2.1.6 2-*N*-Piperidinopyrimidine (L6)

The reaction of 2-chloropyrimidine with piperidine in an ethanolic solution gave 77% yield of 2-*N*-piperidinopyrimidine (**L6**), a yellowish brown liquid. The infrared spectrum of compound **L6** showed medium absorption bands at 1586 cm^{-1} and 1545 cm^{-1} which were due to C=N and C=C stretchings respectively. A strong absorption band was also observed at 2933 cm^{-1} , which was due to C-H stretching. The mass spectrum showed a $[M^+]$ peak at m/z 163 corresponding to the molecular formula $C_9H_{13}N_3$.



L6

The $^1\text{H-NMR}$, $^{13}\text{C-NMR}$ spectra of **L6** are as in the appendix. The $^1\text{H-NMR}$ spectrum of **L6** showed a doublet at δ 8.27 with coupling constant of 4.6 Hz, which was due to H_4 and H_6 of pyrimidine ring. A triplet at δ 6.40 with J value of 4.9 Hz was due to H_5 of the pyrimidine ring. A multiplet which was recorded at δ 3.78, was due to proton resonance at $H_{2\theta}$ and $H_{6\theta}$ of piperidine ring. A multiplet peak which was observed at δ 1.56 δ 1.65 was assigned to $H_{3\alpha}$, $H_{4\theta}$ and $H_{5\theta}$ of piperidine ring.

The $^{13}\text{C-NMR}$ spectrum of **L6** indicated the presence of 9 carbon atoms which is in agreement with the molecular formula of $C_9H_{13}N_3$. A very low intensity absorption peak recorded at δ 161.70 was due to C_2 of the pyrimidine ring. An absorption peak at δ 157.70 was assigned to C_4 and C_6 of pyrimidine ring. A medium absorption peak at δ 108.99, was due to C_5 of the pyrimidine ring. In the upfield region, absorption peaks

were observed between δ 44.76 ó δ 24.88 which corresponds to the carbons of the piperidine ring. One peak at δ 44.76 was assigned to C_{2ø} and C_{6ø} of piperidine ring. A strong absorption peak at δ 25.73 was due to C_{3ø} and C_{5ø} of piperidine ring. An absorption peak at δ 24.88 was assigned to C_{4ø} of the piperidine ring. The full proton and carbon assignments were summarized in Table 2.10.

Table 2.10: ¹H-NMR and ¹³C-NMR chemical shifts of 2-*N*-piperidinopyrimidine (L6)

Proton / Carbon Number Assignments	Chemical Shift in ppm (δ) ^a	
	¹ H-NMR	¹³ C-NMR
2	-	161.70
4	8.27 (d, 2H)	157.70
5	6.40 (t, 1H)	108.99
6	8.27 (d, 2H)	157.70
2ø	3.78 (m, 4H)	44.76
3ø	1.56 ó 1.65(m, 6H)	25.73
4ø	1.56 ó 1.65 (m, 6H)	24.88
5ø	1.56 ó 1.65 (m, 6H)	25.73
6ø	3.78 (m, 4H)	44.76

^a d = doublet, t = triplet, m = multiplet

2.2 Characterization of the Copper Complexes

Each of the ligand molecules (**L1** – **L4**) acts in a monodentate manner coordinating through the pyrimidyl nitrogen and is a binuclear complex. In the crystal structure of all complexes, the four acetate groups each bridge a pair of Cu(II) atoms. The coordination of the metal atoms is distorted octahedral, with the bonding O atoms comprising a square basal plane and is completed by an N atom derived from the ligand and the second Cu atom. Intramolecular N-H...O hydrogen bonding is present between the imino and carboxy groups in all complexes. All the four complexes gave satisfactory C, H and N analyses as shown in Table 2.11. A comparative study of the infrared spectral data of the complexes with those of the free ligands supported the evidence of coordination between the metal and the ligand.

Table 2.11 : Analytical data and some physical properties for complexes CuL1, CuL2, CuL3 and CuL4

	Complex			
	CuL1	CuL2	CuL3	CuL4
Formula	C ₂₀ H ₃₀ N ₆ O ₈ Cu ₂	C ₂₈ H ₃₀ N ₆ O ₈ Cu ₂	C ₃₀ H ₃₄ N ₆ O ₈ Cu ₂	C ₃₀ H ₃₄ N ₆ O ₈ Cu ₂
Geometry	Distorted octahedral	Distorted octahedral	Distorted octahedral	Distorted octahedral
Colour	Blue	Blue	Blue	Blue
Melting Point (°C)	208 ó 212	206 ó 210	188 ó 202	214 ó 218
C ^a (%)	38.98 (38.42)	47.58 (47.67)	49.25 (49.12)	49.13 (49.12)
H ^a (%)	4.72 (4.92)	3.92 (4.29)	4.36 (4.67)	4.38 (4.67)
N ^a (%)	13.51 (13.78)	12.07 (11.91)	11.32 (11.46)	11.24 (11.46)

^a Found (calcd)%.

2.2.1 Tetra- μ -acetato- κ^8 O:O'-bis{[N-ethylpyrimidin-2-amine]copper(II)}(CuL1)

Treatment of ligand **L1** with copper(II) acetate in acetonitrile and trimethylorthoformate (TMOF) gave 62% yield. The infrared absorptions of the free ligand, **L1** and the title compound, **CuL1** were compared as shown in Table 2.12. The band at 478 cm^{-1} was assigned to Cu δ N stretching vibration (Roy, *et al.*, 2007). In the free ligand, a medium absorption band was observed indicating the presence of aromatic C=C stretching at 1534 cm^{-1} but there is a shift to 1541 cm^{-1} in **CuL1**. A shift of $\nu_{\text{(C=Npyrim)}}$ from 1595 cm^{-1} in the free ligand to 1585 cm^{-1} in the complex was consistent with coordination of pyrimidine nitrogen (Chattopadhyay, *et al.*, 1997). **L1** showed an absorption band of medium intensity at 3258 cm^{-1} which was due to N δ H stretching but shifted to lower wavenumber in its copper complex, **CuL1**, to suggest Cu δ N bonding (Masoud, *et al.*, 1994).

Table 2.12 : Infrared spectral data for 2-N-ethylaminopyrimidine (L1) and its copper complex, CuL1

Band Assignments ^a (cm^{-1})	Compound	
	L1	CuL1
(N δ H)	3258m	3323s
(C δ H)	2970s, 2872m	2970s, 2882m
(C=N)	1595m	1585m
(C=C)	1534m	1541s
(Cu δ N)	δ	478s

^a s = strong, m = medium

Recrystallization of **CuL1** in acetonitrile gave prismatic blue crystals which were analyzed by X-ray diffraction. The crystal **CuL1** crystallizes in the triclinic system, *P* space group with the unit cell parameters, $a = 7.8488(6) \text{ \AA}$, $b = 8.5114(7) \text{ \AA}$, $c = 10.2999(8) \text{ \AA}$, $\alpha = 98.404(1)^\circ$, $\beta = 92.698(1)^\circ$ and $\gamma = 105.599(1)^\circ$. In the crystal structure of tetra- μ -acetato- $\kappa^8 O:O'$ -bis{[*N*-ethylpyrimidin-2-amine]copper(II)} (**CuL1**), the four acetate groups each bridge a pair of Cu(II) atoms. The copper(II) ion (Cu1) has a distorted octahedral geometry with the square basal plane formed by four oxygen atoms (O1, O2, O3 and O4) of acetate groups and the apical positions are occupied by the coordinating nitrogen atom of the pyrimidine ring (N1) and Cu1 δ Cu1 interaction at 2.6540(4) \AA . The crystal system and refinement data are shown in Table 2.13.

Table 2.13 : Crystal data and structure refinement for tetra- μ -acetato- $\kappa^8 O:O'$ -bis{[*N*-ethylpyrimidine-2-amine]copper(II)} (CuL1**)**

Empirical formula	Cu ₂ (C ₂ H ₃ O ₂) ₄ (C ₆ H ₉ N ₃) ₂
Formula weight (g mol ⁻¹)	609.58
Colour	Blue
Crystal system, space group	Triclinic, <i>P</i>
Unit cell dimensions	$a = 7.8488(6) \text{ \AA}$ $b = 8.5114(7) \text{ \AA}$ $c = 10.2999(8) \text{ \AA}$ $\alpha = 98.404(1)^\circ$ $\beta = 92.698(1)^\circ$ $\gamma = 105.599(1)^\circ$
$V (\text{\AA}^3)$	652.92 (9)
Z	1
$P_{\text{calc.}}$ (mg m ⁻³)	1.550
Absorption coefficient (mm ⁻¹)	1.68
F_{000}	314
Crystal size (mm)	0.40 x 0.35 x 0.10
θ_{max}	2.5 δ 28.2
$\ddot{O}h \ddot{O}$	-10 to 10
$\ddot{O}k \ddot{O}$	-11 to 11
$\ddot{O}l \ddot{O}$	-13 to 13
Reflections collected / unique	6208/ 2969
R_{int}	0.018
Data / restraints / parameters	2969/ 1/ 170
Goodness-of-fit on F^2	1.02
Final R indices [$I > 2\sigma(I)$]	0.026
R indices (all data)	0.080

The coordination sphere of Cu(II) is a slightly distorted octahedral with the equatorial Cu δ O bond distances varying from 1.953(1) to 1.978(2) Å and the axial Cu δ N(1) distance of 2.246(2) Å. The O δ Cu δ O angles vary from 88.86(8) to 89.76(8) $^\circ$ and from 166.94(6) to 167.23(6) $^\circ$, whereas the O δ Cu δ N angles vary from 93.54(6) to 99.52(6) $^\circ$. The *N*-heterocycle is effectively planar as seen in the C8 δ N3 δ C9 δ C10 torsion angle of -166.6(2) $^\circ$. An intramolecular N3 δ H \cdots O1 interaction contributes to the stability of the dinuclear molecule. In the crystal packing, the presence of C δ H \cdots O interactions connect dinuclear molecules into supramolecular chains along the *b* axis as illustrated in Figure 2.5 and Table 2.15. A thermal ellipsoid of tetra- μ -acetato- κ^8 O:O'-bis{[*N*-ethylpyrimidin-2-amine]copper(II)} (**CuL1**) at the 50% probability level showing the numbering scheme is given in Figure 2.4 with selected bond distances and angles in Table 2.14.

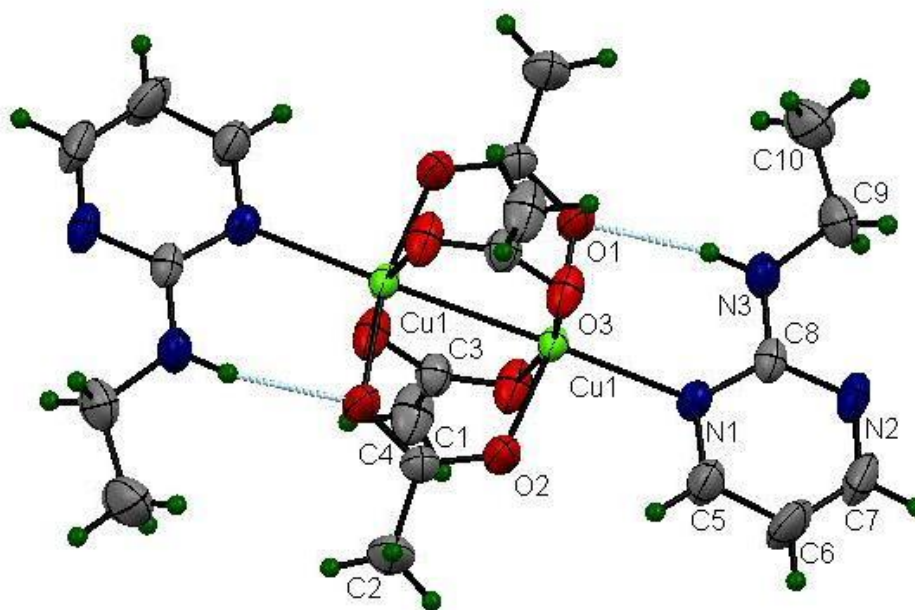


Figure 2.4 : ORTEP diagram of tetra- μ -acetato- κ^8 O:O'-bis{[*N*-ethylpyrimidin-2-amine]copper(II)} (CuL1**)**

Table 2.14 : Selected bond lengths (Å) and angles (°) for tetra- μ -acetato- κ^8 O':O'-bis{[N-ethyl-pyrimidine-2-amine]copper(II)} (CuL1)

Atoms	Length
Cu16O1	1.978 (2)
Cu16O2	1.963 (2)
Cu16O3	1.955 (1)
Cu16O4	1.953 (1)
Cu16N1	2.246 (2)
Cu16Cu1	2.654 (4)
Atoms	Angle
O46Cu16O3	167.23 (6)
O46Cu16O2	88.86 (8)
O36Cu16O2	89.53 (8)
O46Cu16O1	89.76 (6)
O36Cu16O1	88.95 (7)
O26Cu16O1	166.94 (6)
O46Cu16N1	97.38 (6)
O36Cu16N1	95.36 (6)
O26Cu16N1	93.54 (6)
O16Cu16N1	99.52 (2)

Symmetry code: (i) $\delta x + 1, \delta y + 1, \delta z + 1$

Table 2.15 : Hydrogen-bond geometry (Å, °) for tetra- μ -acetato- κ^8 O':O'-bis{[N-ethyl-pyrimidine-2-amine]copper(II)} (CuL1)

$D \delta H \cdots A$	$D \delta H$	$H \cdots A$	$D \cdots A$	$D \delta H \cdots A$
N36H3...O1	0.85 (1)	2.04 (1)	2.871 (2)	164 (2)
C46H4...O3	0.96	2.51	3.458 (3)	171

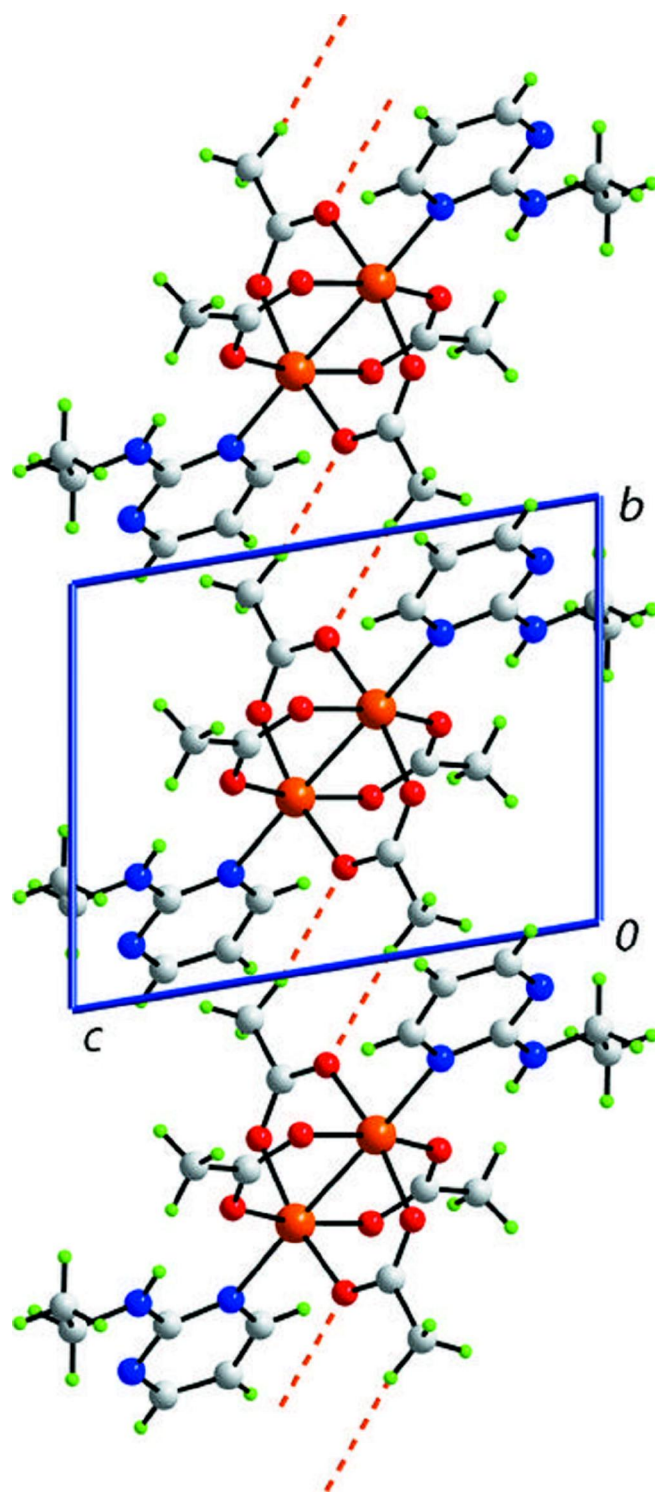


Figure 2.5 : Supramolecular array of tetra- μ -acetato- κ^8 O 2 -bis
 {[N-ethylpyrimidin-2-amine]copper(II)} (CuL1) in the *bc* plane

2.2.2 Tetra- μ -acetato- κ^8 O:O'-bis{[N-(pyrimidin-2-yl)aniline- κ N]copper(II)}(CuL2)

A greenish blue solution of copper(II) acetate in acetonitrile was added dropwise to a solution of ligand **L2** in the same solvent. After several days, a dark blue precipitate was formed and was then recrystallized from acetonitrile to give 68% yield of blue crystals **CuL2** suitable for x-ray crystallography.

The infrared absorptions of the free ligand, **L2** and the title compound, **CuL2** were compared as shown in Table 2.16. The presence of a band at 494 cm^{-1} was assignable to Cu δ N stretching vibration (Roy, *et al.*, 2007). An absorption band was observed in the free ligand indicating the presence of aromatic C=C stretches at 1537 cm^{-1} but there is a shifting in wavenumber to 1572 cm^{-1} in **CuL2**. The (C=N_{py}m) band observed at 1578 cm^{-1} in the free ligand was shifted towards higher wavenumber by 19 cm^{-1} , indicating involvement of the pyrimidyl nitrogen (N1) in coordination (Akyuz, 2009). An absorption band at 3258 cm^{-1} in the free ligand due to N δ H stretching also shifted to 3316 cm^{-1} in its copper complex, **CuL2**.

Table 2.16 : Infrared spectral data for 2-N-anilinopyrimidine (L2) and its copper complex, CuL2

Band Assignments ^a (cm ⁻¹)	Compound	
	L2	CuL2
(N δ H)	3258m	3316s
(C δ H)	3054w	3058w
(C=N)	1578s	1597m
(C=C)	1537s	1572s
(Cu δ N)	δ	494w

^a s = strong, m = medium, w = weak

The X-ray structural investigation of tetra- μ -acetato- $\kappa^8 O:O'$ -bis{[*N*-(pyrimidin-2-yl)aniline- κN]copper(II)} (**CuL2**) shows that the ligand is monodentate with the pyrimidyl nitrogen involved in coordination with the copper atom. This compound crystallizes in the monoclinic system, $P2_1/n$ space group with the unit cell parameters, $a = 11.1241(5)$ Å, $b = 7.3563(4)$ Å, $c = 17.8546(9)$ Å and $\beta = 100.927(5)$ Å. This complex is found to adopt a distorted octahedral copper environment comprising one nitrogen donor atom from the ligand (N1) and the second Cu atom at the apical position and four oxygen atoms (O1, O2, O3 and O4) from the acetate groups. The crystal system and refinement data are shown in Table 2.17.

Table 2.17 : Crystal data and structure refinement for tetra- μ -acetato- $\kappa^8 O:O'$ -bis{[*N*-(pyrimidin-2-yl)aniline- κN]copper(II)} (CuL2**)**

Empirical formula	Cu ₂ (O ₂ C ₂ H ₃) ₄ (C ₁₁ H ₁₁ N ₃) ₂
Formula weight (g mol ⁻¹)	703.64
Colour	Blue
Crystal system, space group	Monoclinic, $P2_1/n$
Unit cell dimensions	$a = 11.1241(5)$ Å $b = 7.3563(4)$ Å $c = 17.8546(9)$ Å $\alpha = 90^\circ$ $\beta = 100.927(5)^\circ$ $\gamma = 90^\circ$
V (Å ³)	1434.59 (12)
Z	2
P_{calc} (mg m ⁻³)	1.629
Absorption coefficient (mm ⁻¹)	2.36
F_{000}	720
Crystal size (mm)	0.35 x 0.35 x 0.15
Öh Ö	-13 to 13
Ök Ö	-9 to 9
Öl Ö	-22 to 22
Reflections collected / unique	5442/ 4909
R_{int}	0.049
Data / restraints / parameters	4909/ 202
Goodness-of-fit on F^2	1.06
Final R indices [$I > 2\sigma(I)$]	0.074
R indices (all data)	0.201

The binuclear unit has a center of symmetry located between two copper ions. The Cu δ Cu distance within the binuclear unit is 2.6092(6) Å; the ligand **L2** acts as a monodentate ligand with nitrogen (N1) as coordinating atom. The equatorial Cu δ O bond distances vary from 1.9663(18) to 1.9858(17) Å and the axial Cu δ N(1) distance is 2.180(2) Å. The O δ Cu δ O angles vary from 88.14(8) to 90.46(8) $^\circ$ and from 169.04(7) to 169.15(8) $^\circ$, whereas the O δ Cu δ N angles vary from 93.81(7) to 97.03(7) $^\circ$. An ORTEP diagram of tetra- μ -acetato- κ^8 O:O'-bis{[N-(pyrimidin-2-yl)aniline- κ N]copper(II)} (**CuL2**) at the 50% probability level showing the numbering scheme is given in Figure 2.6 with selected bond distances and angles in Table 2.18. An intramolecular N3 δ H3 δ ...O1 interaction noted is given in Table 2.19.

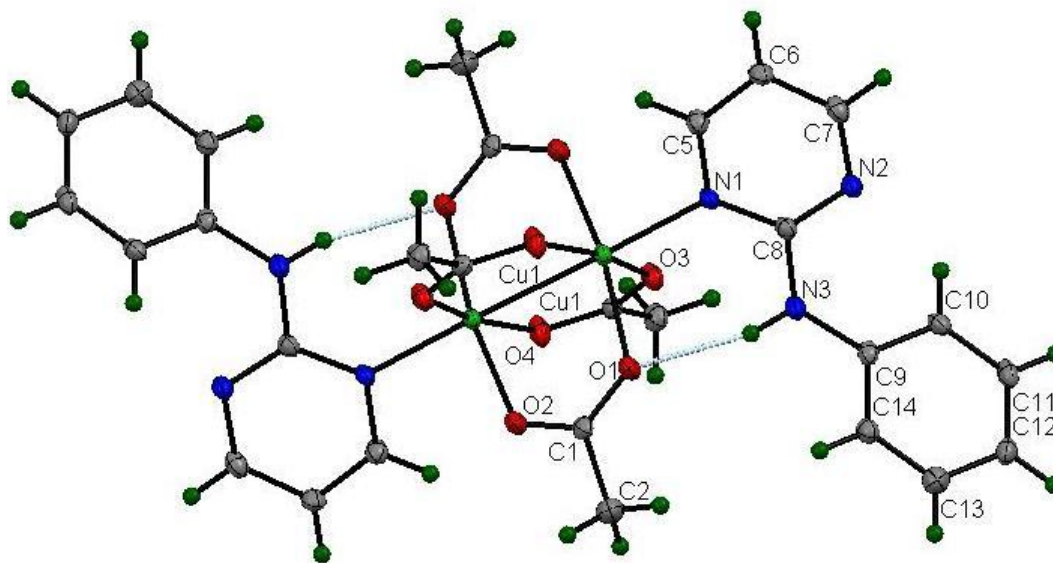


Figure 2.6 : ORTEP diagram of tetra- μ -acetato- κ^8 O:O'-bis{[N-(pyrimidin-2-yl)aniline- κ N]copper(II)} (CuL2**)**

Table 2.18 : Selected bond lengths (Å) and angles (°) for tetra- μ -acetato- $\kappa^8 O:O'$ -bis{[N-(pyrimidin-2-yl)aniline- κN]copper(II)} (CuL2)

Atoms	Length
Cu1óO3	1.9663 (18)
Cu1óO2	1.9858 (17)
Cu1óO4	1.9671 (17)
Cu1óO1	1.9843 (18)
Cu1óN1	2.180 (2)
Cu1óCu1	2.6092 (6)
Atoms	Angle
O3óCu1óO2	89.49 (8)
O3óCu1óO4	169.15 (8)
O2óCu1óO4	89.87 (7)
O3óCu1óO1	88.14 (8)
O2óCu1óO1	169.04 (7)
O4óCu1óO1	90.46 (8)
O3óCu1óN1	97.03 (7)
O2óCu1óN1	94.66 (7)
O4óCu1óN1	93.81 (7)
O1óCu1óN1	96.25 (7)

Symmetry code: (i) $\delta x + 1, \delta y + 1, \delta z + 1$

Table 2.19 : Hydrogen-bond geometry (Å, °) for tetra- μ -acetato- $\kappa^8 O:O'$ -bis{[N-(pyrimidin-2-yl)aniline- κN]copper(II)} (CuL2)

$D \delta H \cdots A$	$D \delta H$	$H \cdots A$	$D \cdots A$	$D \delta H \cdots A$
N3óH3 \cdots O1	0.88	2.08	2.901 (3)	155

2.2.3 Tetra- μ -acetato- κ^8 O:O'-bis{[N-(pyrimidin-2-yl)4-methylaniline- κ N] copper(II)} (CuL3)

Treatment of ligand **L3** with copper(II) acetate dissolved in acetonitrile and trimethylorthoformate (TMOF) gave 66% yield. Copper(II) acetate was added dropwise to a solution of ligand and heated at 50 ó 60°C with continuous stirring. Evaporation of solvent and recrystallization from acetonitrile gave the blue crystals, **CuL3**.

The infrared absorptions of the free ligand, **L3** and the title compound, **CuL3** were compared and as shown in Table 2.20. The presence of a strong absorption band at 442 cm^{-1} was assignable to CuóN stretching vibration (Roy, *et al.*, 2007). The characteristic band of aromatic C=C skeletal stretching at 1534 cm^{-1} in the free ligand shifted to 38 cm^{-1} higher wavelength in **CuL3**. In the free ligand, the (C=N_{py}m) band observed at 1586 cm^{-1} was shifted to 1606 cm^{-1} , indicating coordination *via* nitrogen (N1) (Akyuz, 2009). **L3** showed a medium absorption band at 3258 cm^{-1} which was due to NóH stretching but shifted to higher wavenumber in its copper complex, **CuL3**.

Table 2.20 : Infrared spectral data for 2-N-(*p*-methylanilino)pyrimidine (L3) and its copper complex, CuL3

Band Assignments ^a (cm^{-1})	Compound	
	L3	CuL3
(NóH)	3258m	3325s
(CóH)	2860w	2923w
(C=N)	1586s	1606m
(C=C)	1534s	1572s
(CuóN)	ó	442s

^a s = strong, m = medium, w = weak

The compound, tetra- μ -acetato- $\kappa^8 O:O'$ -bis{[*N*-(pyrimidin-2-yl)4-methylaniline- κN]copper(II)} (**CuL3**) crystallizes in the monoclinic system of $P2_1/c$ space group with the unit cell parameters, $a = 22.329(19)$ Å, $b = 19.923(15)$ Å, $c = 7.476(6)$ Å and $\beta = 107.041(6)$ Å. The distorted octahedral copper coordination environment is completed by four oxygen atoms (O1, O2, O3 and O4) from acetate groups in the square basal plane position, the coordinating nitrogen atom of the pyrimidine ring (N1) and the second Cu atom occupying the apical positions. The crystal system and refinement data are shown in Table 2.21.

Table 2.21 : Crystal data and structure refinement for tetra- μ -acetato- $\kappa^8 O:O'$ -bis{[*N*-(pyrimidin-2-yl) 4-methylaniline- κN]copper(II)} (CuL3)

Empirical formula	Cu ₂ (O ₂ C ₂ H ₃) ₄ (C ₁₁ H ₁₁ N ₃) ₂
Formula weight (g mol ⁻¹)	733.71
Colour	Blue
Crystal system, space group	Monoclinic, $P2_1/c$
Unit cell dimensions	$a = 22.329(19)$ Å $b = 19.923(15)$ Å $c = 7.476(6)$ Å $\beta = 107.041(17)^\circ$
V (Å ³)	3180 (4)
Z	4
P_{calc} (mg m ⁻³)	1.533
Absorption coefficient (mm ⁻¹)	1.40
F_{000}	1512
Crystal size (mm)	0.35 x 0.10 x 0.10
Öh Ö	-26 to 12
Ök Ö	-23 to 23
Öl Ö	-5 to 8
Reflections collected / unique	2683 / 1535
R_{int}	0.071
Data / restraints / parameters	2683/ 211
Goodness-of-fit on F^2	1.20
Final R indices [$I > 2\sigma(I)$]	0.094
R indices (all data)	0.267

The coordination sphere of copper(II) is distorted octahedral with the equatorial Cu δ O bond distances varying from 1.953(8) to 2.006(8) Å and the axial Cu δ N(1) distance of 2.188(8) Å. The O δ Cu δ O angles vary from 88.2(4) to 91.4(3) $^\circ$ and from 164.4(3) to 169.2(3) $^\circ$, whereas the O δ Cu δ N angles vary from 91.4(3) to 99.9(4) $^\circ$. The binuclear unit has a center of symmetry located between the two copper ions. The Cu δ Cu distance within the binuclear unit is 2.649(3) Å. An ORTEP diagram of tetra- μ -acetato- κ^8 O':O'-bis{[N-(pyrimidin-2-yl)4-methylaniline- κ N]copper(II)} (**CuL3**) at the 50% probability level showing the numbering scheme is given in Figure 2.7 with selected bond distances and angles in Table 2.22. An intramolecular N3 δ H3 \cdots O1 interaction noted is given in Table 2.23.

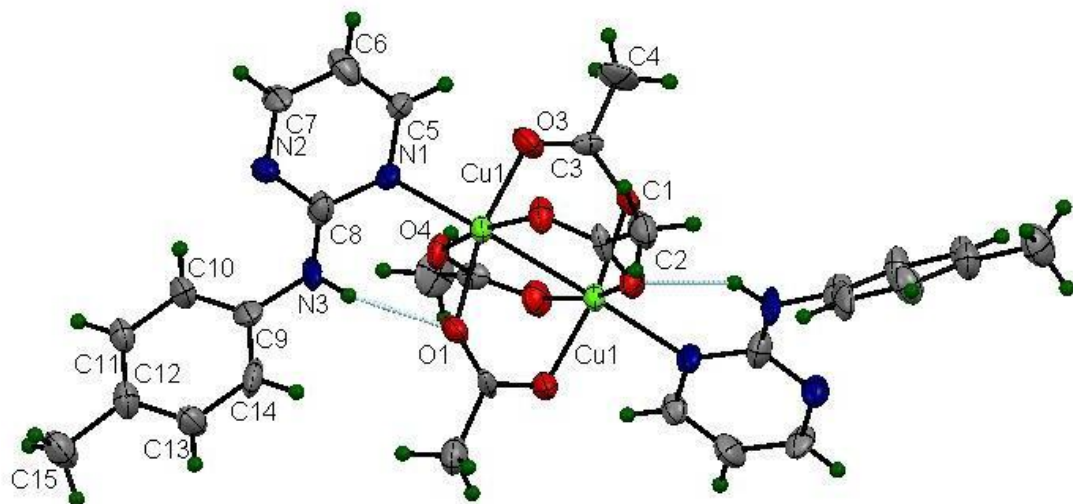


Figure 2.7 : ORTEP diagram of tetra- μ -acetato- κ^8 O':O'-bis{[N-(pyrimidin-2-yl)4-methylaniline- κ N]copper(II)} (**CuL3**)

Table 2.22 : Selected bond lengths (Å) and angles (°) for tetra- μ -acetato- $\kappa^8 O:O'$ -bis{[*N*-(pyrimidin-2-yl)4-methylaniline- κN]copper(II)} (CuL3)

Atoms	Length
Cu16O4	1.953 (8)
Cu16O2	1.958 (8)
Cu16O3	1.967 (9)
Cu16O1	2.006 (8)
Cu16N1	2.188 (8)
Cu16Cu1	2.649 (3)
Atoms	Angle
O46Cu16O2	169.2 (3)
O46Cu16O3	88.2 (4)
O26Cu16O3	89.1 (4)
O46Cu16O1	88.4 (3)
O26Cu16O1	91.4 (3)
O36Cu16O1	164.4 (3)
O46Cu16N1	99.4 (4)
O26Cu16N1	91.4 (3)
O36Cu16N1	99.9 (4)
O16Cu16N1	95.6 (3)

Symmetry code: (i) $\delta x + 1, y, \delta z + \frac{1}{2}$

Table 2.23 : Hydrogen-bond geometry (Å, °) for tetra- μ -acetato- $\kappa^8 O:O'$ -bis{[*N*-(pyrimidin-2-yl)4-methylaniline- κN]copper(II)} (CuL3)

<i>D</i> δ H... <i>A</i>	<i>D</i> δ H	H... <i>A</i>	<i>D</i> ... <i>A</i>	<i>D</i> δ H... <i>A</i>
N36H3...O1	0.86	2.08	2.850 (12)	149

2.2.4 Tetra- μ -acetato- $\kappa^8 O:O'$ -bis{[N-(pyrimidin-2-yl)3-methylaniline- κN]copper(II)} (CuL4)

Tetra- μ -acetato- $\kappa^8 O:O'$ -bis{[N-(pyrimidin-2-yl)3-methylaniline- κN]copper(II)} (**CuL4**) was obtained when a mixture of **L4** and copper(II) acetate, in acetonitrile was heated at 50 ó 60°C with continuous stirring. After several days at room temperature, the dark blue precipitate, formed, and recrystallized from acetonitrile to give 42% of blue crystals, **CuL4**.

The infrared absorptions of the free ligand, **L4** and the title compound, **CuL4** were compared as recorded in Table 2.24. A strong absorption band was observed at 500 cm^{-1} in **CuL4** was assignable to CuóN stretching (Roy, *et al.*, 2007). In the free ligand, an absorption band was observed indicating the presence of aromatic C=C stretching at 1534 cm^{-1} but there is a shift to 1572 cm^{-1} in **CuL4**. The $_{(C=N_{\text{pym}})}$ band observed at 1573 cm^{-1} in the free ligand was shifted 1601 cm^{-1} while an absorption band at 3257 cm^{-1} in the free ligand due to NóH stretching also shifted to 3293 cm^{-1} in its copper complex, **CuL4**.

Table 2.24 : Infrared spectral data for 2-N-(*m*-methylanilino)pyrimidine (L4) and its copper complex, CuL4

Band Assignments ^a (cm^{-1})	Compound	
	L4	CuL4
(NóH)	3257m	3293s
(CóH)	3022w	3023w
(C=N)	1573s	1601w
(C=C)	1534s	1572m
(CuóN)	ó	500s

^a s = strong, m = medium, w = weak

Tetra- μ -acetato- $\kappa^8 O:O'$ -bis{[*N*-(pyrimidin-2-yl)3-methylaniline- κN]copper(II)} (**CuL4**) has similar structural features to the previous three complexes in which the copper atom adopts a distorted octahedral geometry comprising one nitrogen atom from the monodentate pyrimidine ligand (N1) and the second Cu atom at the apical positions and is completed with four oxygen atoms of acetate groups (O1, O2, O3 and O4), each bridging a pair of copper atoms. This compound crystallizes in the triclinic system, *P* space group with the unit cell parameters, $a = 7.5971(8) \text{ \AA}$, $b = 10.5220(11) \text{ \AA}$, $c = 11.1769(12) \text{ \AA}$, $\alpha = 66.1200(10)^\circ$, $\beta = 85.688(2)^\circ$ and $\gamma = 77.693(2)^\circ$. The crystal system and refinement data are shown in Table 2.25.

Table 2.25 : Crystal data and structure refinement for tetra- μ -acetato- $\kappa^8 O:O'$ -bis{[*N*-(pyrimidin-2-yl) 3-methylaniline- κN]copper(II)} (CuL4**)**

Empirical formula	Cu ₂ (O ₂ C ₂ H ₃) ₄ (C ₁₁ H ₁₁ N ₃) ₂
Formula weight (g mol ⁻¹)	733.71
Colour	Blue
Crystal system, space group	Triclinic, <i>P</i>
Unit cell dimensions	$a = 7.5971(8) \text{ \AA}$ $b = 10.5220(11) \text{ \AA}$ $c = 11.1769(12) \text{ \AA}$ $\alpha = 66.1200(10)^\circ$ $\beta = 85.688(2)^\circ$ $\gamma = 77.693(2)^\circ$
$V (\text{\AA}^3)$	798.13 (15)
Z	1
$P_{\text{calc.}}$ (mg m ⁻³)	1.527
Absorption coefficient (mm ⁻¹)	1.39
F_{000}	378
Crystal size (mm)	0.25 x 0.25 x 0.05
$\text{\AA}h \text{\AA}$	-9 to 9
$\text{\AA}k \text{\AA}$	-13 to 13
$\text{\AA}l \text{\AA}$	-14 to 14
Reflections collected / unique	7545/ 3633
R_{int}	0.029
Data / restraints / parameters	3633/ 1/ 215
Goodness-of-fit on F^2	1.04
Final R indices [$I > 2\sigma(I)$]	0.038
R indices (all data)	0.111

The coordination sphere of Cu(II) is a slightly distorted octahedron with the equatorial CuóO bond distances varying from 1.958(2) to 1.9801(18) Å and the axial CuóN(1) distance of 2.204(2) Å. The OóCuóO angles vary from 88.85(9) to 90.46(10)° and from 168.16(8) to 168.34(8)°, whereas the OóCuóN angles vary from 93.64(8) to 98.17(8)°. The CuóCu distance within the binuclear unit is 2.6216(6) Å. An ORTEP diagram of tetra- μ -acetato- $\kappa^8 O:O'$ -bis{[*N*-(pyrimidin-2-yl)3-methylaniline- κN]copper(II)} (**CuL4**) at the 50% probability level showing the numbering scheme is given in Figure 2.8 with selected bond distances and angles in Table 2.26. An intramolecular N3óH3...O1 interaction noted is given in Table 2.27.

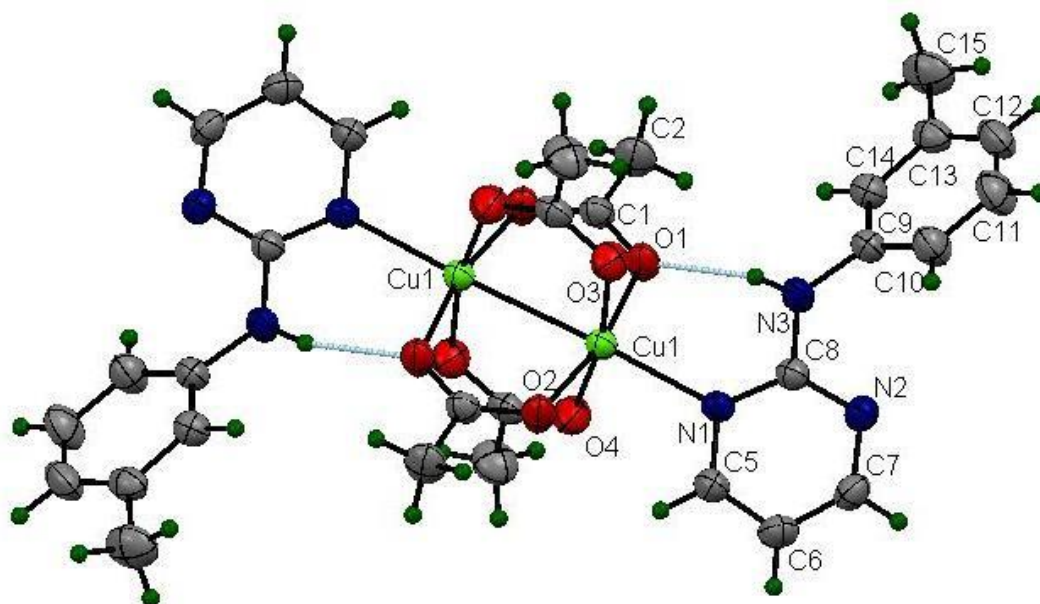


Figure 2.8 : ORTEP diagram of tetra- μ -acetato- $\kappa^8 O:O'$ -bis{[*N*-(pyrimidin-2-yl)3-methylaniline- κN]copper(II)} (**CuL4**)

Table 2.26 : Selected bond lengths (Å) and angles (°) for tetra- μ -acetato- $\kappa^8 O:O'$ -bis{[N-(pyrimidin-2-yl)3-methylaniline- κN]copper(II)} (CuL4)

Atoms	Length
Cu16O4	1.958 (2)
Cu16O3	1.963 (19)
Cu16O2	1.971 (19)
Cu16O1	1.980 (18)
Cu16N1	2.204 (2)
Cu16Cu1	2.6216 (6)
Atoms	Angle
O46Cu16O3	168.34 (8)
O46Cu16O2	90.46 (10)
O36Cu16O2	88.90 (9)
O46Cu16O1	89.40 (9)
O36Cu16O1	88.85 (9)
O26Cu16O1	168.16 (8)
O46Cu16N1	94.77 (8)
O36Cu16N1	96.88 (8)
O26Cu16N1	93.64 (8)
O16Cu16N1	98.17 (8)

Symmetry code: (i) $\delta x + 1, \delta y + 1, \delta z + 1$

Table 2.27 : Hydrogen-bond geometry (Å, °) for tetra- μ -acetato- $\kappa^8 O:O'$ -bis{[N-(pyrimidin-2-yl)3-methylaniline- κN]copper(II)} (CuL4)

$D \delta H \cdots A$	$D \delta H$	$H \cdots A$	$D \cdots A$	$D \delta H \cdots A$
N36H3 \cdots O1	0.860 (10)	2.069 (13)	2.910 (3)	166 (3)

2.3 Fluorescence Studies of Ligands

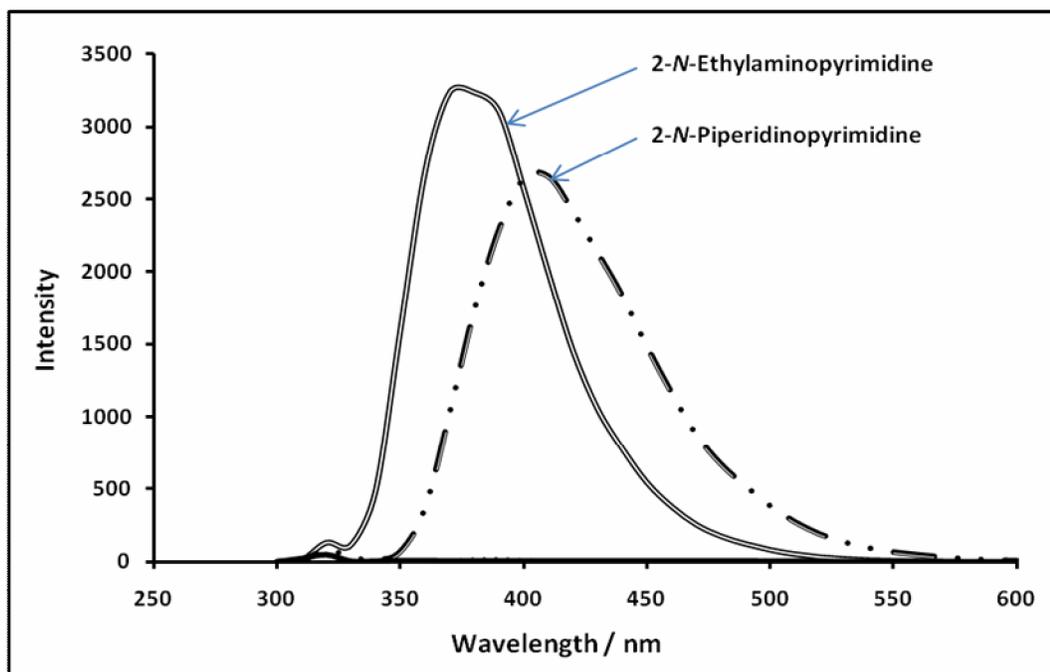
The fluorescence characteristics for each ligand were studied in methanol and DMSO and are summarized in Table 2.28.

Table 2.28 : Fluorescence characteristics of pyrimidine derivatives in capped and uncapped conditions in methanol and DMSO ($M \approx 2.5 \times 10^{-4} \text{ mol dm}^{-3}$)

Compound	Condition	Fluorescence Spectra (nm)					
		Methanol			DMSO		
		E_x	E_m	Intensity	E_x	E_m	Intensity
2- <i>N</i> -Ethylaminopyrimidine (L1)	Capped	324	385	3238	320	379	1781
	Uncapped	324	376	3190	320	379	1643
2- <i>N</i> -Anilinopyrimidine (L2)	Capped	321	353	8.738	318	450	181.0
	Uncapped	321	352	7.471	318	448	170.5
2- <i>N</i> -(<i>p</i> -Methylanilino)pyrimidine (L3)	Capped	334	368	11.35	321	461	45.33
	Uncapped	334	367	9.537	321	461	44.98
2- <i>N</i> -(<i>m</i> -Methylanilino)pyrimidine (L4)	Capped	349	386	10.97	323	454	131.5
	Uncapped	349	387	9.208	323	453	127.5
2- <i>N</i> -Methylanilinopyrimidine (L5)	Capped	345	381	11.40	319	488	23.07
	Uncapped	345	382	11.03	319	487	23.00
2- <i>N</i> -Piperidinopyrimidine (L6)	Capped	325	405	2688	325	411	3238
	Uncapped	325	405	2629	325	405	3102

It can be seen in Table 2.28 that capped samples in methanol, 2-*N*-anilinopyrimidine (**L2**) fluoresced at the lowest wavelength i.e. 353 nm when excited at 321 nm. It is also noted that, 2-*N*-(*p*-methylanilino)pyrimidine (**L3**) fluoresced at 368 nm, 2-*N*-methylanilinopyrimidine (**L5**) at 381 nm and 2-*N*-(*m*-methylanilino)pyrimidine (**L4**) at 386 nm when excited at 334 nm, 345 nm and 349 nm respectively. 2-*N*-ethylaminopyrimidine (**L1**) fluoresced at 385 nm when excited at 324 nm while 2-*N*-piperidinopyrimidine (**L6**) fluoresced at a higher wavelength i.e. 405 nm when excited at 325 nm.

The same trend has been observed in uncapped samples, whereby 2-*N*-anilinopyrimidine (**L2**) fluoresced at the lowest wavelength i.e. 352 nm when excited at 321 nm, 2-*N*-(*p*-methylanilino)pyrimidine (**L3**) fluoresced at 367 nm, 2-*N*-methylanilinopyrimidine (**L5**) at 382 nm and 2-*N*-(*m*-methylanilino)pyrimidine (**L4**) at 387 nm when excited at 334 nm, 345 nm and 349 nm respectively. It is also shown that 2-*N*-ethylaminopyrimidine (**L1**) fluoresced at 376 nm when excited at 324 nm while 2-*N*-piperidinopyrimidine (**L6**) fluoresced at the highest wavelength i.e. 405 nm when excited at 325 nm. The fluorescence spectra of pyrimidine derivatives in capped samples in methanol are as shown in Figure 2.9 and 2.10.



* Plotted area for 2-*N*-anilinopyrimidine, 2-*N*-methylanilinopyrimidine, 2-*N*-(*p*-methylanilino)pyrimidine and 2-*N*-(*m*-methylanilino)pyrimidine since the intensity values are very low, therefore have been shown in Figure 2.10

Figure 2.9 : Fluorescence spectrum of 2-*N*-ethylaminopyrimidine (L1**) and 2-*N*-piperidinopyrimidine (**L6**) in capped samples in methanol ($M \approx 2.5 \times 10^{-4} \text{ mol dm}^{-3}$)**

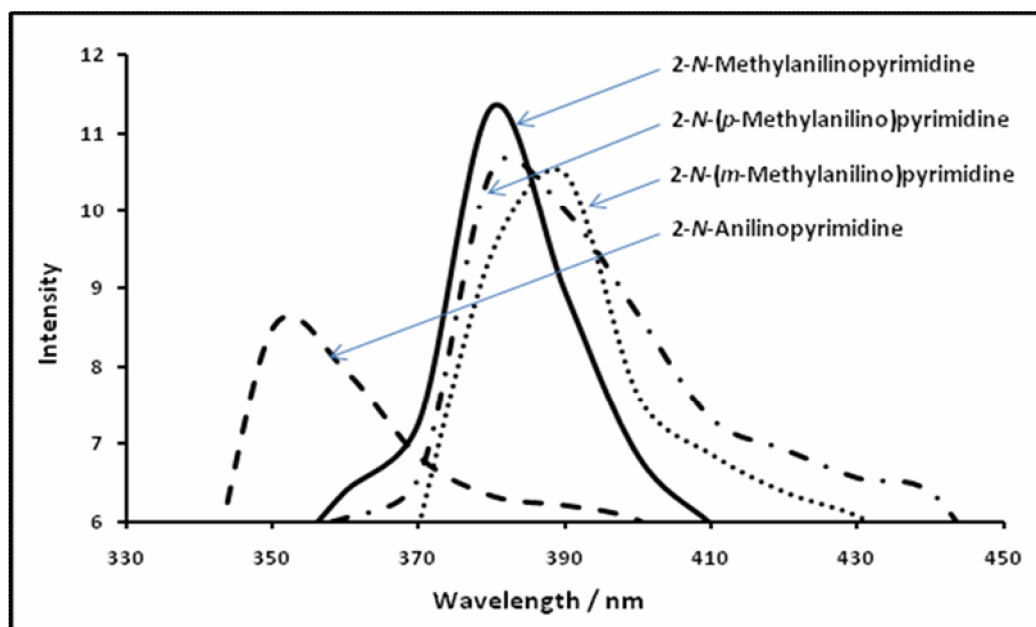


Figure 2.10 : Fluorescence spectrum of 2-*N*-(*p*-methylanilino)pyrimidine (L3), 2-*N*-(*m*-methylanilino)pyrimidine (L4), 2-*N*-methylanilinopyrimidine (L5) and 2-*N*-anilinopyrimidine (L2) in capped samples in methanol ($M \approx 2.5 \times 10^{-4} \text{ mol dm}^{-3}$)

It is also noted that, 2-*N*-ethylaminopyrimidine (L1) showed the highest fluorescence peak in methanol followed by 2-*N*-piperidinopyrimidine (L6), 2-*N*-methylanilinopyrimidine (L5), 2-*N*-(*p*-methylanilino)pyrimidine (L3), 2-*N*-(*m*-methylanilino)pyrimidine (L4) and 2-*N*-anilinopyrimidine (L2). The highest fluorescence intensity observed is believed to be due to the presence of the ethyl group $\delta\text{CH}_2\text{CH}_3$, which is an electron donating substituent. The nature of the ethyl group as an electron donating substituent enhances the mobility of electrons in the system. The free mobility of the electron enhances the $\pi \rightarrow \pi^*$ transitions, thus high fluorescence intensity was observed. Furthermore, the lower fluorescence intensity observed with 2-*N*-piperidinopyrimidine (L6) in methanol compared to 2-*N*-ethylaminopyrimidine (L1) is believed to be due to the piperidino ring flipping from one conformation to another as suggested in Figure 2.11. The flipping of the piperidino ring resulted in the loss of energy in the transition state and consequently low fluorescence intensity is observed (Abdullah, *et al.*, 2004).

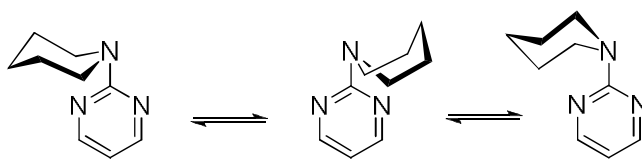


Figure 2.11 : Flipping of piperidino ring in 2-*N*-piperidinopyrimidine (L6)

However, 2-*N*-piperidinopyrimidine (**L6**) is found to be more fluorescent compared to anilino ring substituted compounds, such as 2-*N*-anilinopyrimidine (**L2**), 2-*N*-(*p*-methylanilino)pyrimidine (**L3**), 2-*N*-(*m*-methylanilino)pyrimidine (**L4**) and 2-*N*-methylanilinopyrimidine (**L5**). This is probably due to the rigidity of the structure of 2-*N*-piperidinopyrimidine (**L6**) as shown in Figure 2.12, whereby 2-*N*-piperidinopyrimidine (**L6**) has no $\delta\text{NH}\delta$ bridge as compared to anilino ring substituted compounds. Normally a rigid structure reduces the vibrational amplitudes which promotes radiationless losses which increase the fluorescence intensity.

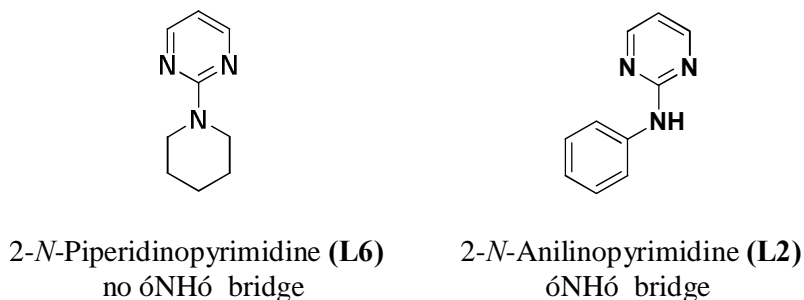


Figure 2.12 : Structures of 2-*N*-piperidinopyrimidine (L6) and 2-*N*-anilinopyrimidine (L2)

On the other hand, 2-*N*-anilinopyrimidine (**L2**), 2-*N*-(*p*-methylanilino)pyrimidine (**L3**), 2-*N*-(*m*-methylanilino)pyrimidine (**L4**) and 2-*N*-methylanilinopyrimidine (**L5**), which have an anilino ring, have non-rigid structures, which are capable of decreasing the fluorescence intensity due to the vibrational amplitudes. The lower fluorescence intensity observed with 2-*N*-anilinopyrimidine (**L2**) in methanol compared to its methyl

substituted compounds, such as 2-*N*-(*p*-methylanilino)pyrimidine (**L3**), 2-*N*-(*m*-methylanilino)pyrimidine (**L4**) and 2-*N*-methylanilinopyrimidine (**L5**) is believed to be due to the nature of the methyl group itself. Methyl group, as an electron donating group, is known to have tendency to enhance the mobility of electrons in a system, thus increasing the fluorescence intensity.

It is also can be seen in Table 2.28 that, under both conditions, capped and uncapped samples in DMSO, fluorescence peaks of 2-*N*-methylanilinopyrimidine (**L5**), 2-*N*-(*p*-methylanilino)pyrimidine (**L3**), 2-*N*-(*m*-methylanilino)pyrimidine (**L4**) and 2-*N*-anilinopyrimidine (**L2**) were shifted by about 70 ó 100 nm to higher wavelengths than in methanol when excited around 318 ó 323 nm. It is also noted that, in capped samples, 2-*N*-anilinopyrimidine (**L2**) fluoresced at 450 nm, 2-*N*-(*p*-methylanilino)pyrimidine (**L3**) fluoresced at 461 nm, 2-*N*-(*m*-methylanilino)pyrimidine (**L4**) at 454 nm and 2-*N*-methylanilinopyrimidine (**L5**) at 488 nm when excited at 318 nm, 321 nm, 323 nm and 319 nm respectively, while in uncapped samples, the same trend has been observed, whereby 2-*N*-anilinopyrimidine (**L2**) fluoresced at 448 nm, 2-*N*-(*p*-methylanilino)pyrimidine (**L3**) fluoresced at 461 nm, 2-*N*-(*m*-methylanilino)pyrimidine (**L4**) at 453 nm and 2-*N*-methylanilinopyrimidine (**L5**) at 487 nm when excited at the same wavelengths as in capped samples respectively.

Higher fluorescence wavelengths observed with 2-*N*-anilinopyrimidine (**L2**), 2-*N*-(*p*-methylanilino)pyrimidine (**L3**), 2-*N*-(*m*-methylanilino)pyrimidine (**L4**) and 2-*N*-methylanilinopyrimidine (**L5**) in DMSO are probably due to the presence of an anilino ring in the system, thus increase the degree of conjugation in the system and therefore allowing the free mobility of electrons within the system (Abdullah, *et al.*,

2004). The same phenomena was observed with pyridine derivatives studied earlier (Bakar, *et al.*, 2006). Consequently, a shift in fluorescence spectra to longer wavelength is usually observed as the polar solvents and dielectric constant increases (Guibault, 1977). This phenomenon favours the shifting of emission maxima towards the higher wavelength. The fluorescence spectra of pyrimidine derivatives in capped samples in DMSO are as shown in Figure 2.13.

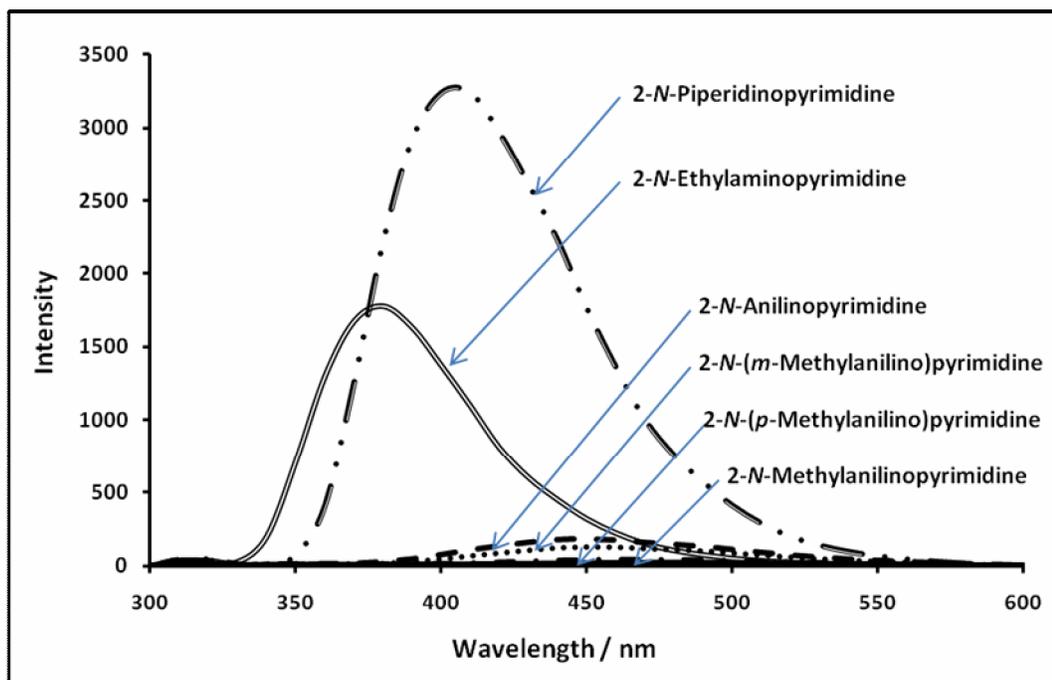


Figure 2.13 : Fluorescence spectrum of pyrimidine derivatives in capped samples in DMSO ($M \approx 2.5 \times 10^{-4} \text{ mol dm}^{-3}$)

The effect of solvents on the fluorescence characteristics of pyrimidine derivatives were studied in only two solvents, methanol, a polar protic solvent and DMSO, a polar aprotic solvent with higher dielectric constant. This is due to the solubility problem. Generally, the fluorescence intensities of pyrimidine derivatives were higher in DMSO compared to methanol. However, 2-*N*-ethylaminopyrimidine (**L1**) showed higher intensity in methanol compared to in DMSO as shown in Figure 2.14.

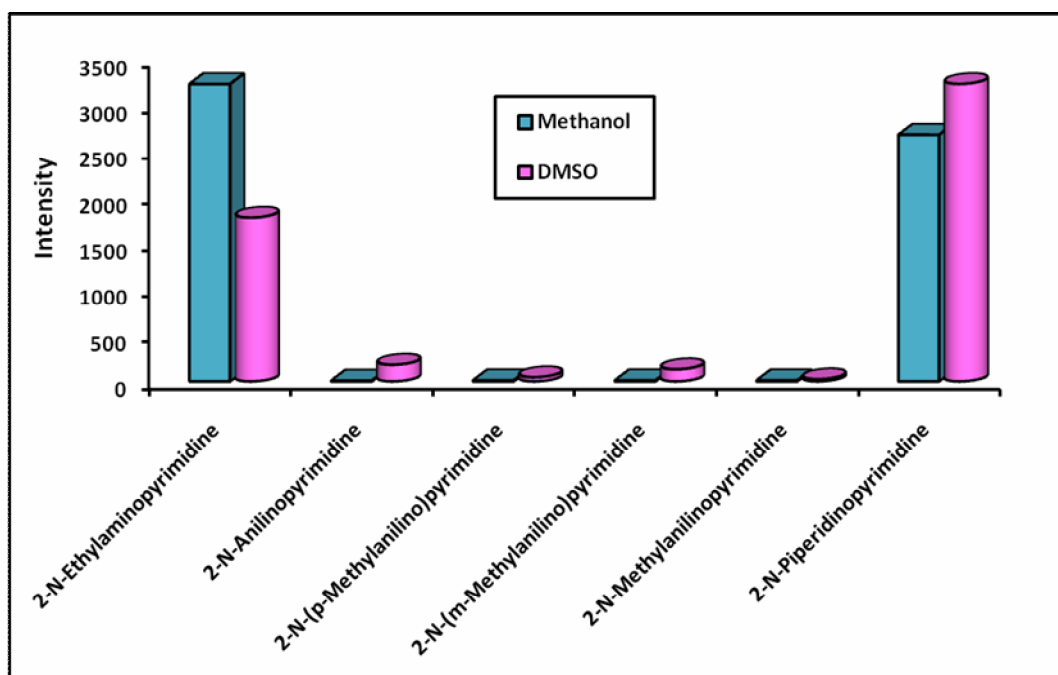


Figure 2.14 : Fluorescence intensities of pyrimidine derivatives in capped samples in methanol and DMSO ($M \approx 2.5 \times 10^{-4} \text{ mol dm}^{-3}$)

The higher intensity in DMSO is believed to be due to the dielectric properties of the solvent. DMSO is a polar aprotic solvent and its polarity produces a greater stabilization of the * excited state, thus increasing the fluorescence intensity. Furthermore, the δCH_3 of methanol may increase the vibrational amplitude of the complex and energy absorbed is thus dissipated as heat and as a result low fluorescence intensity observed. The lowest fluorescence intensity observed in methanol is also believed to be due to the quenching effect from the δ hydrogen bonded solvents associated with the lone pair of electrons on the pyrimidine ring and the amino group. As a result, they are not available to move around the system, thus low fluorescence intensity was observed. It is also believed that the compound formed a complex with the solvent. It shows the formation of intermolecular charge transfer transitions via hydrogen bonding of the compound.

Earlier studies showed that in some aromatic heterocyclic compounds with hydrogen bonding formation would quench the fluorescence intensity (Weisstuch, *et al.*, 1970). The formation of hydrogen bonds capable of conjugating with the electron system of the heterocyclic ring, results in the mobility of the electron being disturbed and causes the fluorescence intensity to be reduced. This phenomenon favours the low lying n → π* transitions which refer to the excitation of a nonbonding electron to an antibonding orbital. It was reported that n → π* transitions were usually not observed in fluorescence spectra and when present were weak (Abdullah, *et al.*, 2004). As a result, a decrease in fluorescence intensity was observed.

However, the high fluorescence intensity observed for 2-*N*-ethylaminopyrimidine (**L1**) in methanol is probably due to hydrogen bonding by the solvent. The maximum intensity observed in this solvent is due to the non-bonding electrons in the solute, that is 2-*N*-ethylaminopyrimidine (**L1**), which is bonded to the hydrogen atom of the solvent, forming a stable hydrogen bonded complex as suggested in Figure 2.15.

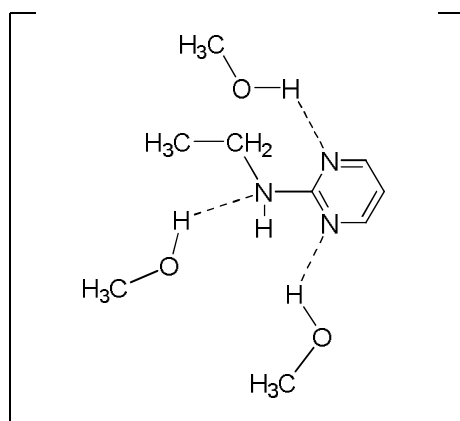


Figure 2.15 : Formation of hydrogen bonded of 2-*N*-ethylaminopyrimidine (L1**)**

This complex stabilizes the ground state as well as the excited state of the $n \rightarrow \pi^*$ transition. However, the ground state of 2-*N*-ethylaminopyrimidine (**L1**) has two electrons in the non-bonding orbital whereas the excited state has only one, therefore the stabilization of the ground state is greater. As the result, the energy of $n \rightarrow \pi^*$ transition increases, thus favouring the low lying $\pi \rightarrow \pi^*$ transition which is responsible for the higher fluorescence intensity (Abdullah, *et al.*, 2004).

It is also noted that, in samples in DMSO, 2-*N*-piperidinopyrimidine (**L6**) showed the highest intensity amongst all the six derivatives of pyrimidine studied as shown in Figure 2.16. There is no clear explanation for this observation because typically, when establishing a solvent-fluorescence relationship, hydrogen bonding, the dielectric constant of the solvent and its viscosity are frequently invoked to explain this relationship (Lippert, *et al.*, 1959, Abdullah, 1989).

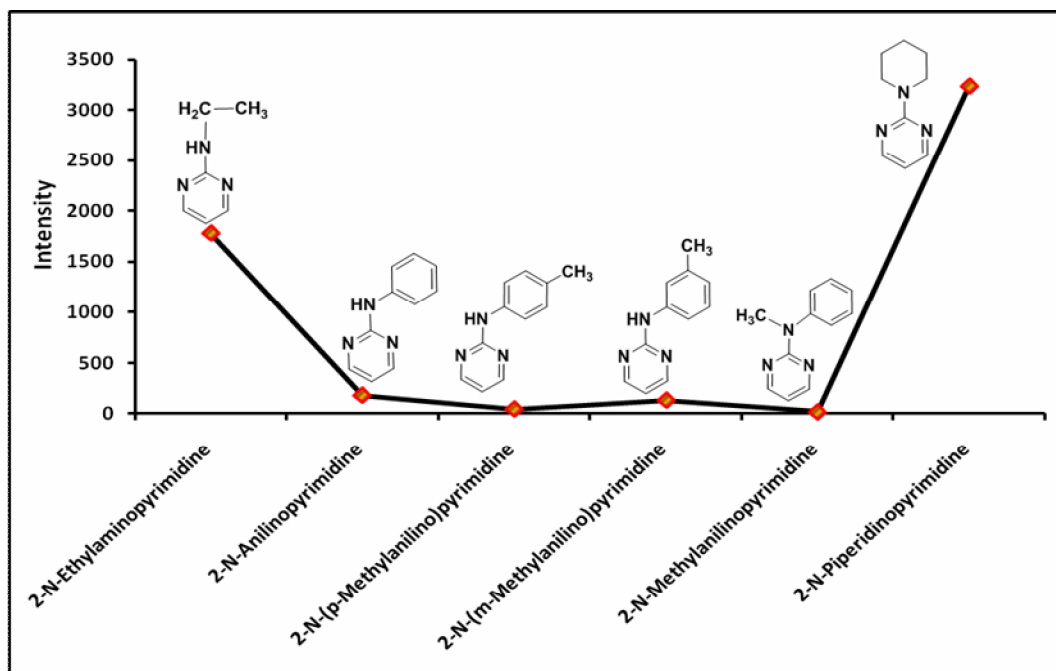


Figure 2.16 : Fluorescence intensities of pyrimidine derivatives in DMSO ($M \approx 2.5 \times 10^{-4} \text{ mol dm}^{-3}$)

The relative intensities for pyrimidine derivatives in DMSO decrease in order 2-*N*-piperidinopyrimidine (**L6**), 2-*N*-ethylaminopyrimidine (**L1**), 2-*N*-anilinopyrimidine (**L2**), 2-*N*-(*m*-methylanilino)pyrimidine (**L4**), 2-*N*-(*p*-methylanilino)pyrimidine (**L3**) and 2-*N*-methylanilinopyrimidine (**L5**). As discussed earlier, electron donating groups tend to enhance the fluorescence intensity due to the electron mobility, therefore 2-*N*-anilinopyrimidine (**L2**) should show the lowest fluorescence intensity compared to its methyl substituted compounds such as 2-*N*-(*m*-methylanilino)pyrimidine (**L4**), 2-*N*-(*p*-methylanilino)pyrimidine (**L3**) and 2-*N*-methylanilinopyrimidine (**L5**). Nevertheless, some experimental results are contradictive to the theoretical expectations. The fluorescence intensity of anilino was higher than its methyl substituted compounds. This result is opposite to the known information that fluorescence intensity increases by introducing electron donating substituent. These exceptions are probably due to the substituent groups that can interact strongly with the solvent. In other words, for aromatic compounds with different functional groups it is impossible to separate structural from environmental effects on their fluorescence behavior.

In general, compounds tend to be fluorescent in polar solvents. Under these conditions, the lone pair of electrons are bonded and the longest absorption wavelength is due to $\pi \rightarrow \pi^*$ transition, instead of $n \rightarrow \pi^*$. The effects of solvent on fluorescence spectra are complex and are due to several factors in addition to solvent polarity. The factors include rate of solvent relaxation, rigidity of the local environment, internal charge transfer, proton transfer and excited state reactions (Lakowicz, 2006). However, it can be difficult to know which effect is dominant in a particular system and typically more than one effect will simultaneously affect the fluorophore.

The effect of air or oxygen on the fluorescence characteristic of pyrimidine derivatives were studied under capped and uncapped conditions in methanol and DMSO. It can be seen in Table 2.28 that, in both solvents, all compounds fluoresced at almost the same wavelength in capped and uncapped samples. However, in capped samples and uncapped samples, all compounds in both solvents showed almost similar fluorescence intensity as shown in Figure 2.17 and Figure 2.18.

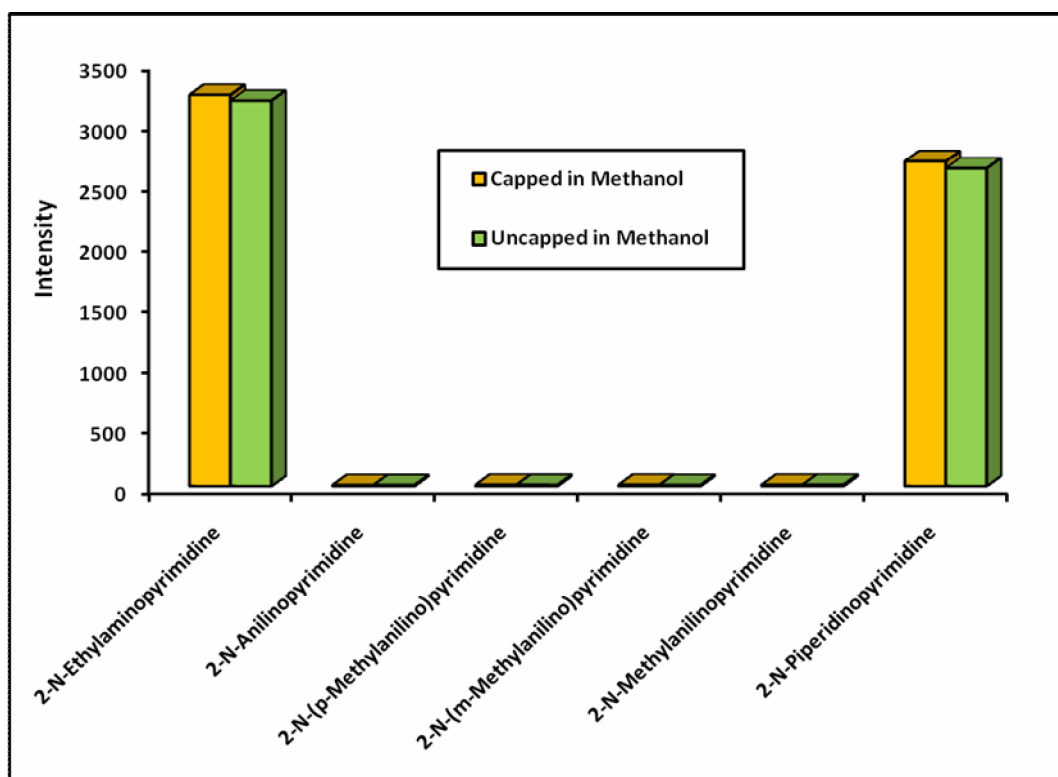


Figure 2.17 : Fluorescence intensities of pyrimidine derivatives in capped and uncapped samples in methanol ($M \approx 2.5 \times 10^{-4} \text{ mol dm}^{-3}$)

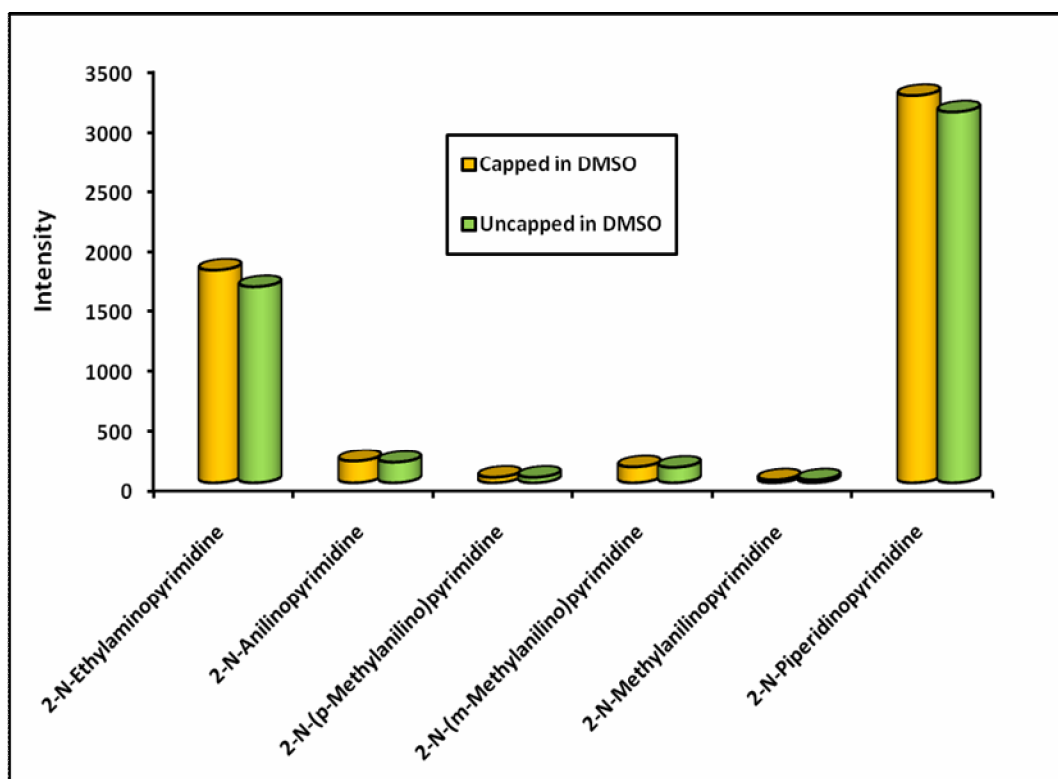


Figure 2.18 : Fluorescence intensities of pyrimidine derivatives in capped and uncapped samples in DMSO ($M \approx 2.5 \times 10^{-4} \text{ mol dm}^{-3}$)

The higher intensity observed in capped samples compared to uncapped samples is believed to be due to the unlimited amount of oxygen or air in the quartz cell, and therefore quenched the fluorescence intensity of the compounds (Haroutounian, *et al.*, 1988). Oxygen, which has an unusually large diffusion coefficient, and on prolong exposure of the solution to the atmosphere, could result in large quantity of oxygen diffusing into solution (Haroutounian, *et al.*, 1995).

2.4 Fluorescence Studies of Copper Complexes

The effect of copper metal on the fluorescence characteristics of the ligands in methanol and DMSO were studied for **L1**, **L2**, **L3** and **L4**. The fluorescence properties of selected pyrimidine derivatives and their copper complexes in methanol and DMSO were compared and the data are summarized in Table 2.29.

Table 2.29 : Fluorescence characteristic of selected pyrimidine derivatives and their copper complexes in methanol and DMSO ($M \approx 2.5 \times 10^{-4} \text{ mol dm}^{-3}$)

Compound	Fluorescence Spectra (nm)					
	Methanol			DMSO		
	E_x	E_m	Intensity	E_x	E_m	Intensity
2- <i>N</i> -Ethylaminopyrimidine (L1)	324	385	3238	320	379	1781
[Cu ₂ (C ₂ H ₃ O ₂) ₄ (C ₆ H ₉ N ₃) ₂] (CuL1)	333	378	3147	323	381	1429
2- <i>N</i> -Anilinopyrimidine (L2)	321	353	8.738	318	450	181.0
[Cu ₂ (C ₂ H ₃ O ₂) ₄ (C ₁₀ H ₉ N ₃) ₂] (CuL2)	328	360	7.340	335	452	212.6
2- <i>N</i> -(<i>p</i> -Methylanilino)pyrimidine (L3)	334	368	11.35	321	461	45.33
[Cu ₂ (C ₂ H ₃ O ₂) ₄ (C ₁₁ H ₁₁ N ₃) ₂] (CuL3)	327	360	10.26	442	507	2.728
2- <i>N</i> -(<i>m</i> -Methylanilino)pyrimidine (L4)	349	386	10.97	323	454	131.5
[Cu ₂ (C ₂ H ₃ O ₂) ₄ (C ₁₁ H ₁₁ N ₃) ₂] (CuL4)	355	393	10.41	non-fluorescent		

It can be seen in Table 2.29 that, both 2-*N*-ethylaminopyrimidine (**L1**) and its copper complex, **CuL1** showed fluorescence peaks between 378 and 385 nm when excited around 320 ó 333 nm in methanol and DMSO as shown in Figure 2.19. The higher fluorescence intensity observed in methanol compared to DMSO is probably due to hydrogen bonding by the solvent as discussed earlier.

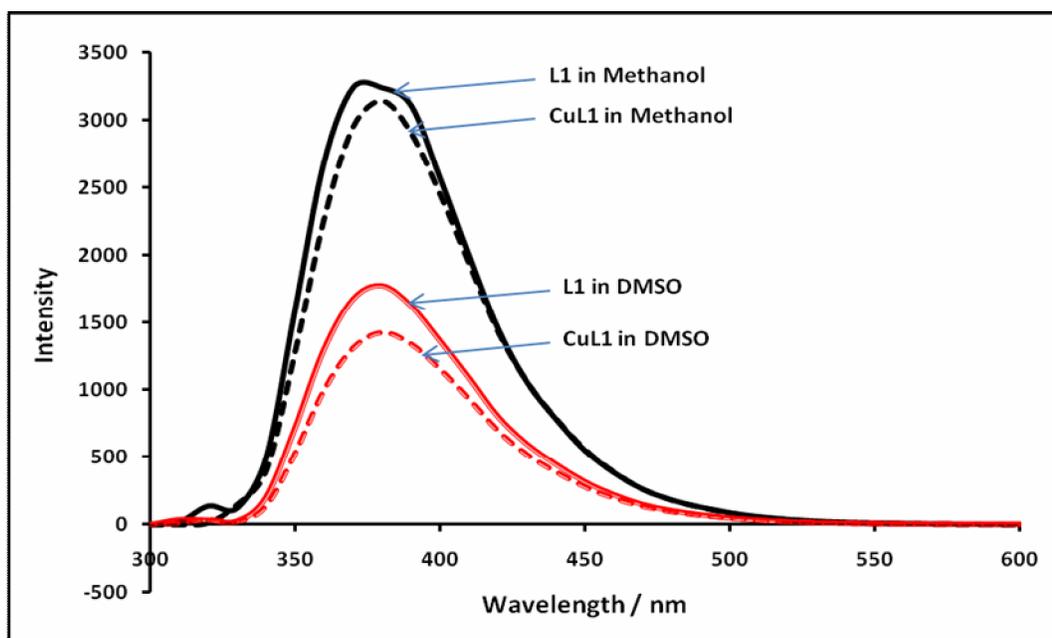


Figure 2.19 : Fluorescence spectra of 2-*N*-ethylaminopyrimidine, L1 and its copper complex, CuL1 in methanol and DMSO ($M \approx 2.5 \times 10^{-4} \text{ mol dm}^{-3}$)

For 2-*N*-anilinopyrimidine (**L2**) and its complex, **CuL2**, the emission peaks were observed at 353 nm and 360 nm when excited at 321 nm and 328 nm in methanol respectively. However, in DMSO, 2-*N*-anilinopyrimidine (**L2**) and its complex, **CuL2** emit about 90 ó 100 nm higher wavelength than in methanol. 2-*N*-(*p*-methylanilino)pyrimidine (**L3**) and its copper complex, **CuL3** showed the same trend as 2-*N*-anilinopyrimidine (**L2**) and its complex, **CuL2** as mentioned earlier, whereby the two fluorescence peaks of 2-*N*-(*p*-methylanilino)pyrimidine (**L3**) and **CuL3** was shifted to higher wavelengths, 461 nm and 507 nm when excited at 321 nm and 442 nm in DMSO respectively, whereas on the other hand in methanol, the fluorescence peaks were observed at 368 nm and 360 nm when excited at 334 nm and 327 nm respectively as shown in Figure 2.20 and 2.21. This is probably due to the presence of an anilino ring in the compounds, thus allowing the free mobility of electron within the system as discussed earlier. Consequently, the fluorescence peaks shifted to higher wavelength.

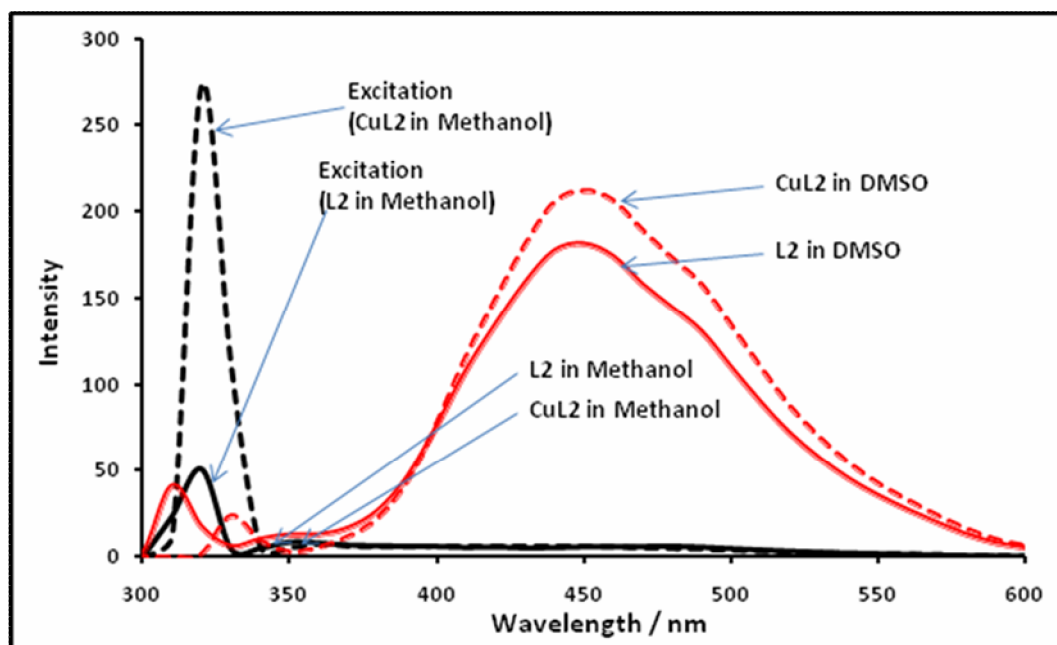


Figure 2.20 : Fluorescence spectra of 2-*N*-anilinopyrimidine, L2 and its copper complex, CuL2 in methanol and DMSO ($M \approx 2.5 \times 10^{-4} \text{ mol dm}^{-3}$)

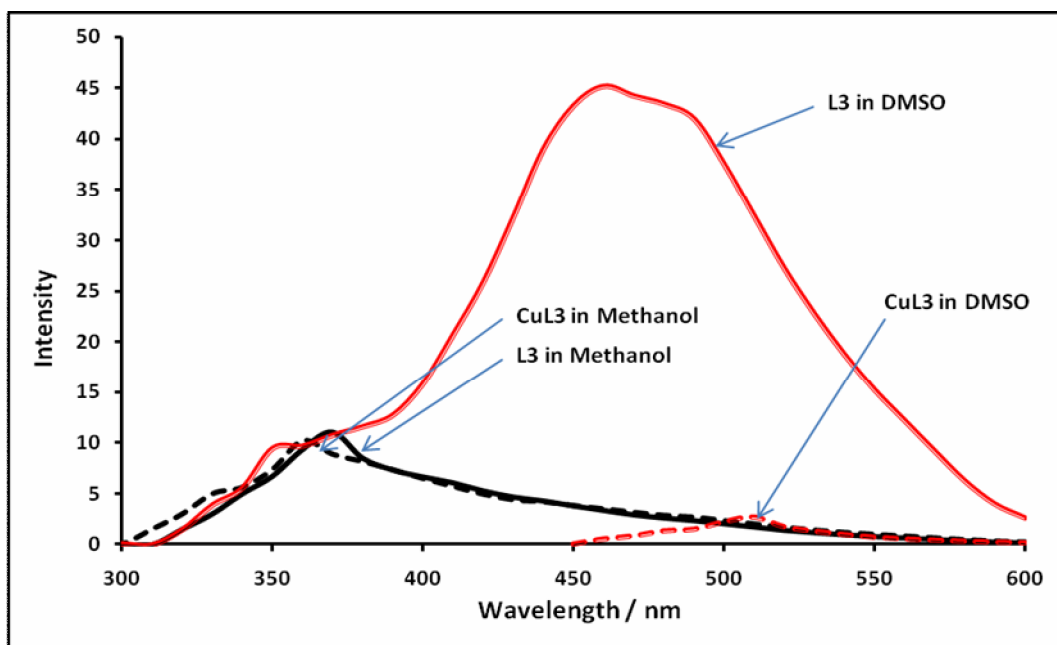


Figure 2.21 : Fluorescence spectra of 2-*N*-(*p*-methylanilino)pyrimidine, L3 and its copper complex, CuL3 in methanol and DMSO ($M \approx 2.5 \times 10^{-4} \text{ mol dm}^{-3}$)

It is also noted that, the fluorescence intensity for 2-*N*-anilinopyrimidine, (**L2**) and its copper complex, **CuL2** in methanol was a very low compared to samples in DMSO. As discussed earlier, the higher fluorescence intensity in DMSO compared to methanol is probably due to the dielectric properties of the solvent, whereby DMSO is a polar aprotic solvent with higher dielectric constant compared to methanol, which is a polar protic solvent with lower dielectric constant value.

2-*N*-(*m*-Methylanilino)pyrimidine (**L4**) and its copper complex, **CuL4**, fluoresced at almost the same wavelength of 386 nm and 393 nm when excited at 349 nm and 355 nm respectively in methanol. On the other hand, in DMSO, the fluorescence peak of 2-*N*-(*m*-methylanilino)pyrimidine (**L4**) was observed at 454 nm when excited at 323 nm while for its copper complex, **CuL4**, no fluorescence peak was observed. The fluorescence spectra for 2-*N*-(*m*-methylanilino)pyrimidine and its copper complexes in methanol and DMSO are given in Figure 2.22.

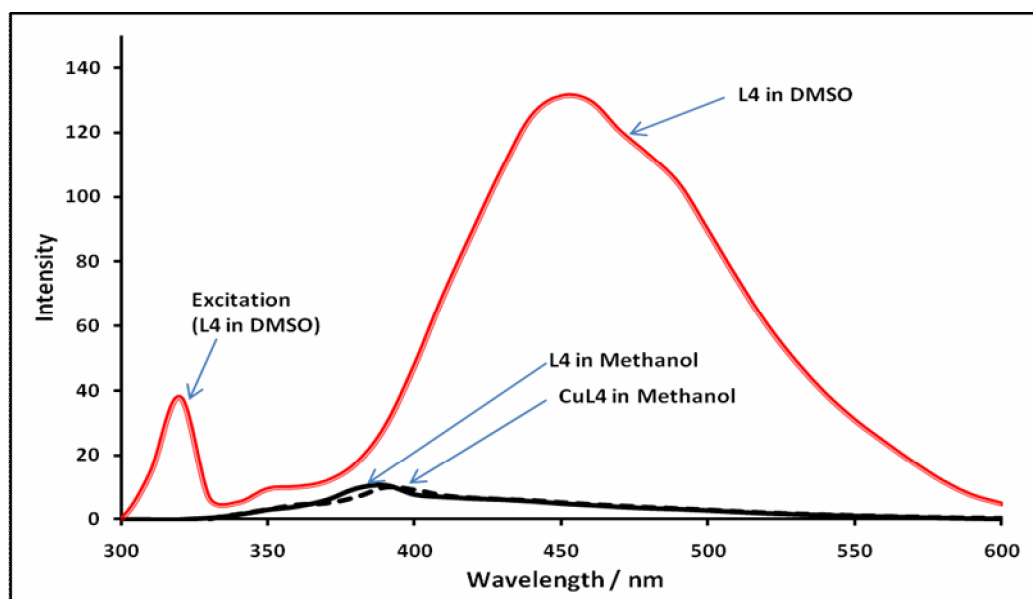
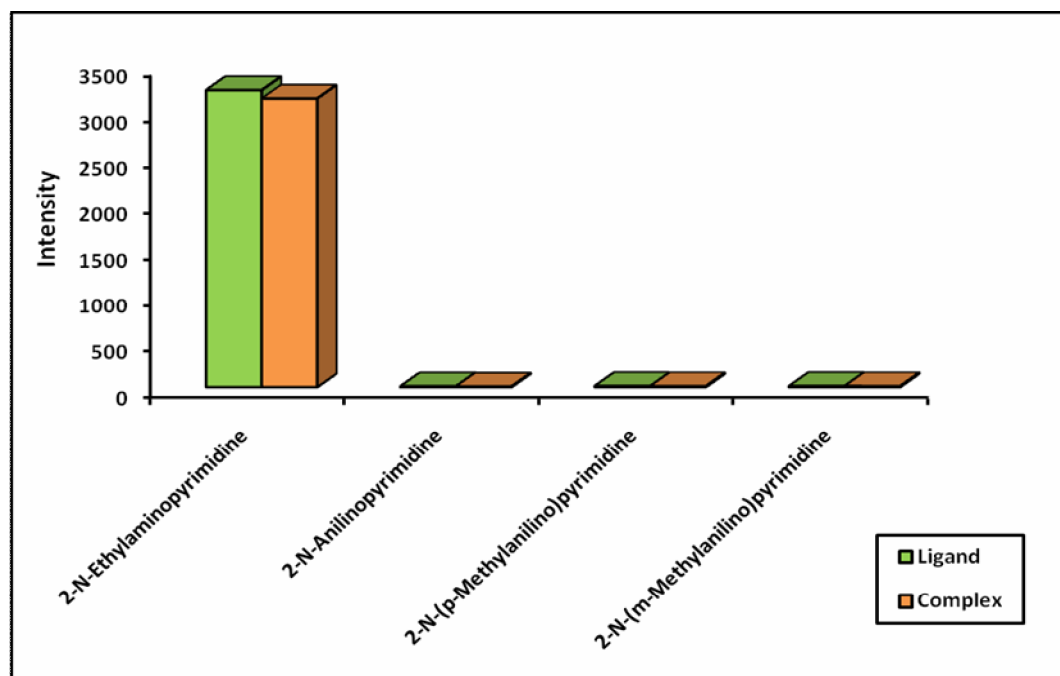


Figure 2.22 : Fluorescence spectra of 2-*N*-(*m*-methylanilino)pyrimidine, L4 and its copper complex, CuL4 in methanol and DMSO ($M \approx 2.5 \times 10^{-4} \text{ mol dm}^{-3}$)

Generally, the intensities of the ligands in both solvents were higher than their copper complexes as shown in Figure 2.23 & 2.25. The higher fluorescence intensity observed for the ligands compared to their copper complexes is probably due to quenching effect of the transition metal, which bound to the ligand during complexation whereby the charge transfer transition occurred between ligand and metal ion (Schulman, 1977). In metal complexes, there is charge transfer from the ligand to metal ions, thus decreasing the relative fluorescence intensity (Aiyub, *et al.*, 2007). The copper complex of 2-*N*-anilinopyrimidine, **CuL2** however, showed an increase in fluorescence intensity compared to its ligand in DMSO. The increases in fluorescence intensity can be explained by the rigid structure of 2-*N*-anilinopyrimidine (**L2**) when it complexes with copper metal ion. As a result the energy absorbed is not lost through vibration, thus higher fluorescence intensity was observed.



* Plotted area for 2-*N*-anilinopyrimidine, 2-*N*-methylanilinopyrimidine and 2-*N*-(*p*-methylanilino)pyrimidine cannot be seen clearly in the Figure 2.23 as the intensity values are very low, therefore has been shown in Figure 2.24

Figure 2.23 : Fluorescence intensities of selected pyrimidine derivatives and their copper complexes in methanol ($M \approx 2.5 \times 10^{-4} \text{ mol dm}^{-3}$)

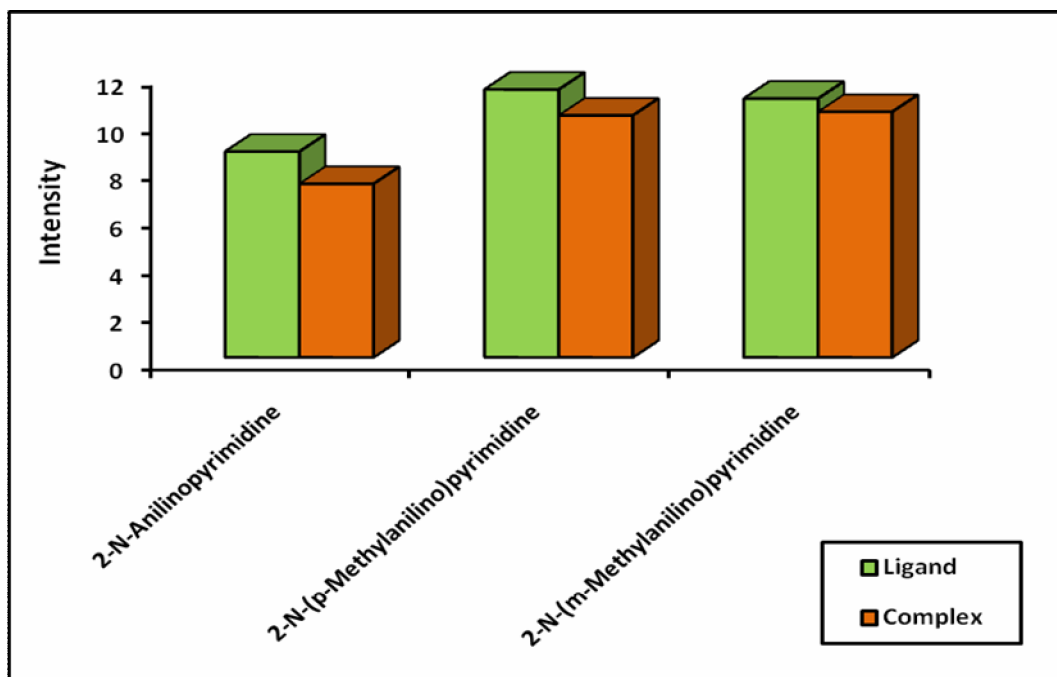


Figure 2.24 : Fluorescence intensities of selected pyrimidine derivatives and their copper complexes in methanol ($M \approx 2.5 \times 10^{-4} \text{ mol dm}^{-3}$)

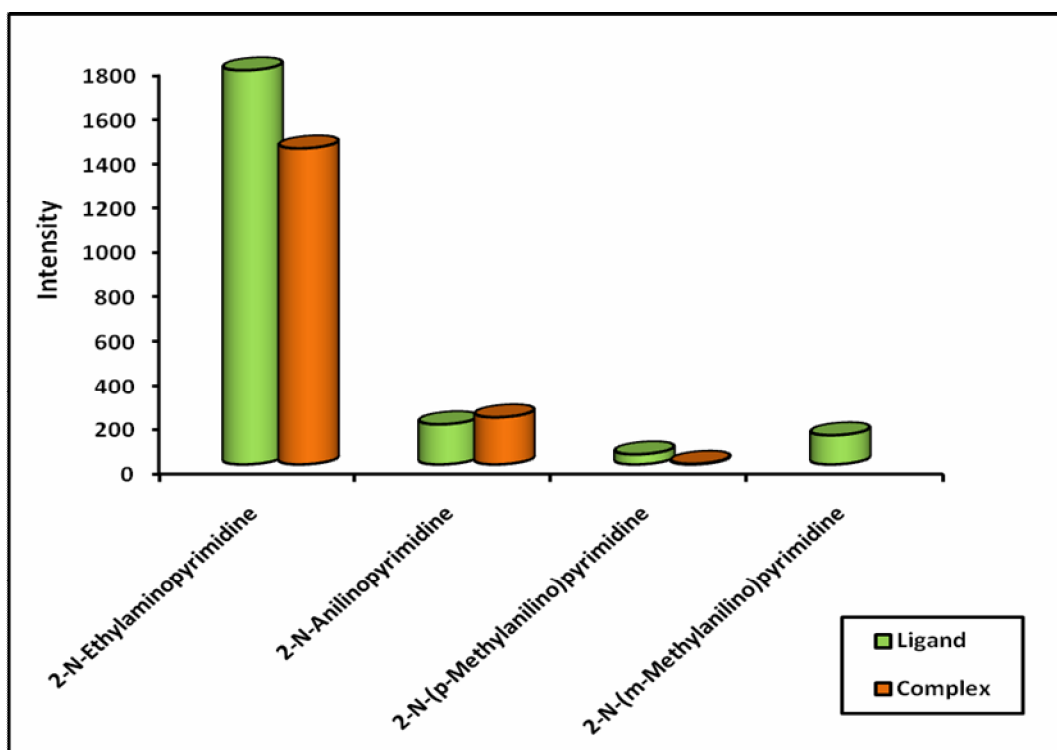


Figure 2.25 : Fluorescence intensities of selected pyrimidine derivatives and their copper complexes in DMSO ($M \approx 2.5 \times 10^{-4} \text{ mol dm}^{-3}$)

It is also noted that, the copper complex of 2-*N*-ethylaminopyrimidine, **CuL1** showed the highest fluorescence intensity in both methanol and DMSO. Since the fluorescence intensity of **CuL1** complex was much higher than that of the other complexes, it can be inferred that the energy difference between the ligand state and the emitting energy state of **CuL1** is more favourable for energy transfer than the other three copper complexes. Usually, metal complexes show a decrease in fluorescence intensities compared to ligands due to the delocalization of π electrons within the system. An increase in fluorescence intensity can be explained by metal to ligand charge transfer when ligand complexes with the metal (Aiyub, *et al.*, 2006).